RESEARCH ARTICLE

PALEONTOLOGY

Early giant reveals faster evolution of large body size in ichthyosaurs than in cetaceans

P. Martin Sander[1,2]*, Eva Maria Griebeler[3]*, Nicole Klein[1], Jorge Velez Juarbe[4], Tanja Wintrich[1,5], Liam J. Revell[6,7], Lars Schmitz[2,8]*

Body sizes of marine amniotes span six orders of magnitude, yet the factors that governed the evolution of this diversity are largely unknown. High primary production of modern oceans is considered a prerequisite for the emergence of cetacean giants, but that condition cannot explain gigantism in Triassic ichthyosaurs. We describe the new giant ichthyosaur *Cymbospondylus youngorum* sp. nov. with a 2-meter-long skull from the Middle Triassic Fossil Hill Fauna of Nevada, USA, underscoring rapid size evolution despite the absence of many modern primary producers. Surprisingly, the Fossil Hill Fauna rivaled the composition of modern marine mammal faunas in terms of size range, and energy-flux models suggest that Middle Triassic marine food webs were able to support several large-bodied ichthyosaurs at high trophic levels, shortly after ichthyosaur origins.

Body size is a fundamental attribute of any organism, and extreme body sizes are of special interest to evolutionary biologists. Gigantism is found in different guises in the terrestrial and marine realms (*1*). Several lineages of mammals and reptiles secondarily adapted to marine habitats and diversified to become species-rich clades (*2*), best exemplified by marine mammals since the Paleogene and by marine reptiles of the Mesozoic. Today, multiple species of cetaceans (toothed whales, or odontocetes, and baleen whales, or mysticetes) and pinnipeds (seals and sea lions) inhabit the pelagic ecosystem and differ in body size, feeding strategy, and trophic level (*3*), ranging from macropredatory raptorial feeding (top of the food chain, e.g., killer whales or orcas, *Orcinus orca*) to filter feeding (low in the food chain, e.g., baleen whales). Large marine mammals, especially cetaceans, have been pivotal components of pelagic food webs since at least the late Paleogene, superseding the ichthyosaurs, plesiosaurs, and mosasaurs of the Mesozoic in this role. Body size appears to be a major axis of the phylogenetic and ecological diversification of secondarily marine amniotes.

[1]Abteilung Paläontologie, Institut für Geowissenschaften, Universität Bonn, 53115 Bonn, Germany. [2]The Dinosaur Institute, Natural History Museum of Los Angeles County, Los Angeles, CA 90007, USA. [3]Institut für Organismische und Molekulare Evolutionsbiologie, Evolutionäre Ökologie, Johannes Gutenberg–Universität Mainz, 55099 Mainz, Germany. [4]Department of Mammalogy, Natural History Museum of Los Angeles County, Los Angeles, CA 90007, USA. [5]Anatomisches Institut, Universität Bonn, 53115 Bonn, Germany. [6]Department of Biology, University of Massachusetts Boston, Boston, MA 02125, USA. [7]Universidad Católica de la Santísima Concepción, Concepción, Chile. [8]W.M. Keck Science Department of Claremont McKenna, Scripps, and Pitzer Colleges, Claremont, CA 91711, USA.
*Corresponding author. Email: martin.sander@uni-bonn.de (P.M.S.); em.griebeler@uni-mainz.de (E.M.G.); lschmitz@kecksci.claremont.edu (L.S.)

Analyses of the evolution of body size in independent lineages of pelagic amniotes offer the promise to improve the understanding of the patterns and processes of adaptation to life in marine environments. Repeated transitions from fully terrestrial to obligate marine habitats document how the anatomy and ecology of each lineage evolved in response to the shift from terrestrial to aquatic habitats. Recurring evolutionary patterns may suggest predictability of ecology as well as physiological constraints to maximum and minimum sizes (*4*, *5*). Ichthyosaurs and cetaceans are among the most prominent lineages to exemplify secondary aquatic adaptations. Both clades offer a well-suited model system to understand size evolution in secondary aquatic adaptation and in the sea in general (*2*).

As tail-propelled pelagic tetrapods, ichthyosaurs and cetaceans not only evolved convergent body shapes, lifestyles, physiologies, and feeding strategies as an adaptation to their habitat, but both lineages also evolved after the near-complete collapse of marine ecosystems. However, emerging evidence suggests different trajectories of body-size evolution in the two groups. Mysticetes shifted from gradual evolution of body size to rapid evolution of exceptionally large body sizes late in the history of the clade, concomitant with the extinction of small species. This pattern is presumed to have been facilitated by abundant resources and coastal upwelling (*6*). By contrast, the morphological disparity, the estimated evolutionary rates of discrete characters, and the evolution of skull size of ichthyosaurs all reached an early peak in the Triassic (*7*). The fast increases in disparity measures in early ichthyosaurs reflect rapid lineage diversification and dietary specialization (*8*), including the first aquatic raptorial tetrapod, *Thalattoarchon*, from the early Middle Triassic Fossil Hill Fauna of Nevada, USA (*8*). The presence of an orca-like predator suggested the emergence of food webs that are more similar to modern webs when compared with preceding Paleozoic webs.

However, the giant body sizes of filter-feeding mysticetes and suction-feeding sperm whales (*Physeter macrocephalus*) seemed out of reach for Early and Middle Triassic ichthyosaurs, especially given the absence of environmental indicators of high productivity such as diatoms, autotrophic dinoflagellates, and coccolithophores (*9*). By increasing the amount of energy available for the higher trophic levels of marine ecosystems, the evolution of these relatively large-bodied, planktonic, primary producers is considered to have been a critical precondition for the emergence of modern giants (*3*, *9*). By contrast, small-bodied plankton probably made up the bulk of the primary producers in Triassic oceans, thus limiting the amount of energy available to large-bodied species at higher trophic levels (*3*). By this logic, one would hypothesize that Triassic marine ecosystems should have fewer large species at high trophic levels than modern faunas.

In this contribution, we combine traditional paleontology with computational trait evolution and food web modeling to compare the patterns of body size evolution of ichthyosaurs and cetaceans in an ecological context (Fig. 1). We describe a new ichthyosaur from the early Middle Triassic Fossil Hill Fauna of Nevada, USA (*10*) as *Cymbospondylus youngorum* sp. nov. (Fig. 2) of giant body size (tables S1 and S2) from well-preserved material. The new ichthyosaur lived close to the beginning of Mesozoic marine reptile evolution as part of the recovery from the end-Permian mass extinction (Fig. 3) 252 million years (Ma) ago. The discovery reinforces the emerging pattern of rapid evolution of body size in ichthyosaurs, which, in contrast to cetaceans, must have experienced their most active phase of size evolution in their early evolutionary history, despite the absence of modern primary producers. We infer that the pelagic ecosystems of the early Middle Triassic (244 Ma ago) could, surprisingly, support several large tetrapod ocean consumers.

Systematic Paleontology

Reptilia Linnaeus, 1758 (*11*)
Diapsida Osborn, 1903 (*12*)
Ichthyosauria Blainville, 1835 (*13*)
Cymbospondylus Leidy, 1868 (*14*)

Type species

Cymbospondylus piscosus Leidy, 1868 (*14*)

Referred species

Cymbospondylus petrinus Leidy, 1868 (*14*); *Cymbospondylus buchseri* (*15*); *Cymbospondylus nichollsi* (*16*); *Cymbospondylus duelferi* (*17*); *Cymbospondylus youngorum* sp. nov.

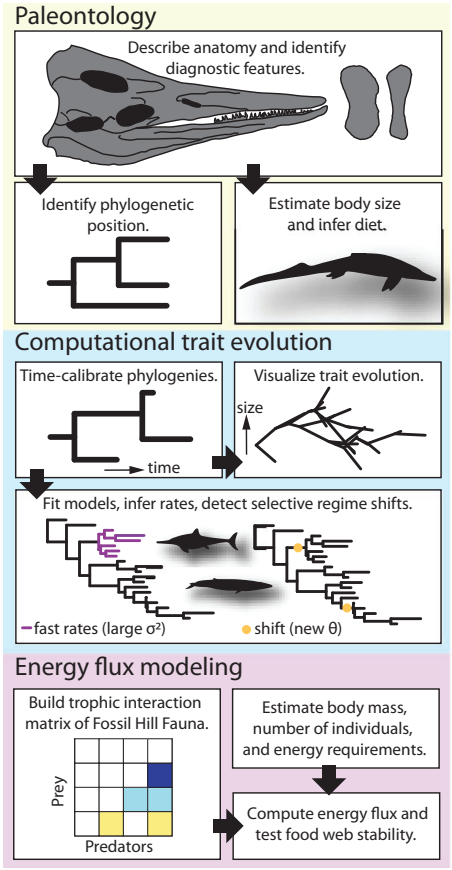

Fig. 1. Conceptual approach of our integrated study. We combine traditional paleontology with computational trait evolution and energy-flux modeling to study macroevolutionary patterns of body size evolution in marine amniotes.

Genus diagnosis

For a recent detailed diagnosis of the genus, see (*17*). In addition, the results of the phylogenetic analysis in this study offer an apomorphy-based diagnosis.

Cymbospondylus youngorum sp. nov. (Fig. 2 and figs. S1 to S5)

Etymology

The species is named in honor of Tom and Bonda Young.

Holotype and only specimen

LACM DI 157871 is the holotype and, as of now, the only recognized individual. LACM DI 157871 is largely articulated and complete from the anterior of the trunk region to the skull, preserved ventral side up. The cervical column back to the middle dorsal vertebrae is present with ribs in articulation. The shoulder girdle is articulated, and the two humeri are situated close to their respective glenoid. At present, the skull (Fig. 2, A to F; figs. S1 and S2; and table S1), the right humerus (Fig. 2, G to K), parts of the shoulder girdle (fig. S3), and some vertebrae are prepared (fig. S3)

Horizon and locality

LACM DI 157871 comes from the Anisian age Fossil Hill Member of the Favret Formation at Favret Canyon, Augusta Mountains, Pershing County, Nevada, USA. The type locality, LACM 8025, is on the northern slope of the rear of Favret Canyon at an elevation of 1676 m. Exact coordinates are on file at the repository. LACM DI 157871 originates from the same general level as the holotype of the macropredatory ichthyosaur *Thalattoarchon saurophagis* (*8*) and the pistosaur *Augustasaurus hagdorni* (*10*) in the lower third of the Fossil Hill member and pertains to the middle Anisian *Taylori* Zone (*18*).

Diagnosis

C. youngorum sp. nov. is diagnosed by a unique combination of the following eight characters (see data S1 for character descriptions and data S3 for a list of synapomorphies): squamosal, participates in supratemporal fenestra (character 72, state 0; Fig. 2); dentary, labial shelf present (character 117, state 1; fig. S2C); angular, extent of anterior lateral exposure is extensive, at least as high and anteriorly as the surangular's exposure (character 120, state 1; Fig. 2); angular, extent of posterior lateral exposure is extensive, with surangular exposure reduced to a thin strip on the lateral surface of the retroarticular process (character 121, state 1; Fig. 2); lower jaw glenoid, deeply excavated and present (character 126, state 1; Fig. 2); dentition, definition of the base of the enamel layer is well defined and precise (character 147, state 1; fig. S2, E and F); humerus, anterior flange is absent (character 200, state 0; Fig. 2 and fig. S6); and humerus, relative anteroposterior width in dorsal view, excluding dorsal and ventral processes, is approximately equal or the proximal end is wider than the distal end (character 206, state 1; Fig. 2 and fig. S6).

The new taxon is characterized by the following autapomorphies: a thick base of bone of attachment of the teeth (Fig. 2 and fig. S2, C and E), the distinctive shape of the scapula with a very large and wide dorsal blade and a narrow ventral part (figs. S3 and S6), the distinctive humerus morphology with a wider proximal than distal end, and a triangular proximal head and triangular shaft cross section (Fig. 2 and fig. S6). Note that these autapomorphies were not added as characters to our character matrix. A differential diagnosis and detailed anatomical descriptions (figs. S2 and S3) and comparisons (figs. S4 to S6 and tables S2 and S3) are provided in the supplementary materials (*10*).

Phylogenetic position

Phylogenetic analyses (*10*) (table S4) indicate that *C. youngorum* sp. nov. is nested within a clade of closely related *Cymbospondylus* species that account for much of the lineage diversity and morphological disparity of large-bodied Early and Middle Triassic ichthyosaurs (Fig. 3 and fig. S7). The close relationship of these species points to an adaptive radiation (as much as one can be recognized in the fossil record of Mesozoic reptiles). Further evidence for such a radiation is that there are no other four seemingly sympatric species of any ichthyosaur genus in the ichthyosaur record and that other finds of *Cymbospondylus* from the late Early and early Middle Triassic are widely distributed across the Northern Hemisphere (*16*).

Our analysis with TNT (a software for phylogenetic analysis) and its "new technology" search algorithm resulted in a tree length of 1225 steps. The four most parsimonious trees were retained (table S4), and the nearly fully resolved strict consensus of the four trees is shown in Fig. 3 and fig. S7. The consistency index of this tree is 0.259, coupled with a retention index of 0.627. The absolute Bremer support of the nodes varies from 1 to 5 (fig. S7). Additional analyses (table S4) confirmed the placement of LACM DI 157871 in a clade with other cymbospondylids, yet the position of the *Cymbospondylus* clade varies with the selection of taxa that were included in the analyses (*10*). We note that the interrelationships of ichthyosaurs remain difficult to resolve, both in the Triassic and the Jurassic part of the tree. This uncertainty reflects the difficulty in resolving ichthyosaur interrelationships in general (*19*) and the need for a concerted effort of redefining and rescoring characters.

Inferred diet and estimated body size

The conical, bluntly pointed tooth crowns of *C. youngorum* sp. nov., in conjunction with the elongate snout, suggest a generalist diet of fish and squid (*20*), as inferred for most ichthyosaurs from teeth and stomach contents (*21*). Considering its size, *C. youngorum* sp. nov. could also have preyed on smaller and juvenile marine reptiles (*10*). The right lower jaw of *C. youngorum* sp. nov. measures 1970 mm from the tip of the dentary to the end of the retroarticular process (table S1). At a total length of 1890 mm (table S1), the skull of LACM DI 15787 is one of the largest complete ichthyosaur skulls known. Although post-Triassic ichthyosaurs never reached the size of Triassic ones again (*7*), there are skulls of *Temnodontosaurus* from the Lower Jurassic of England and Germany (*22*) that are the same length as that of LACM DI 15787 within the limits of preservation. However, these large ichthyosaurs probably were less than 9 m long, having proportionally larger skulls (*22*). Larger skulls than those of LACM DI 15787 and these largest *Temnodontosaurus* specimens are only known from Late Triassic ichthyosaurs, specifically *Shonisaurus popularis* and *Shastasaurus sikanniensis*, with estimated skull lengths of 2750 and 3000 mm, respectively (*7*).

Humerus length is another commonly used proxy for ichthyosaurian body size [(*16*, *17*, *23*);

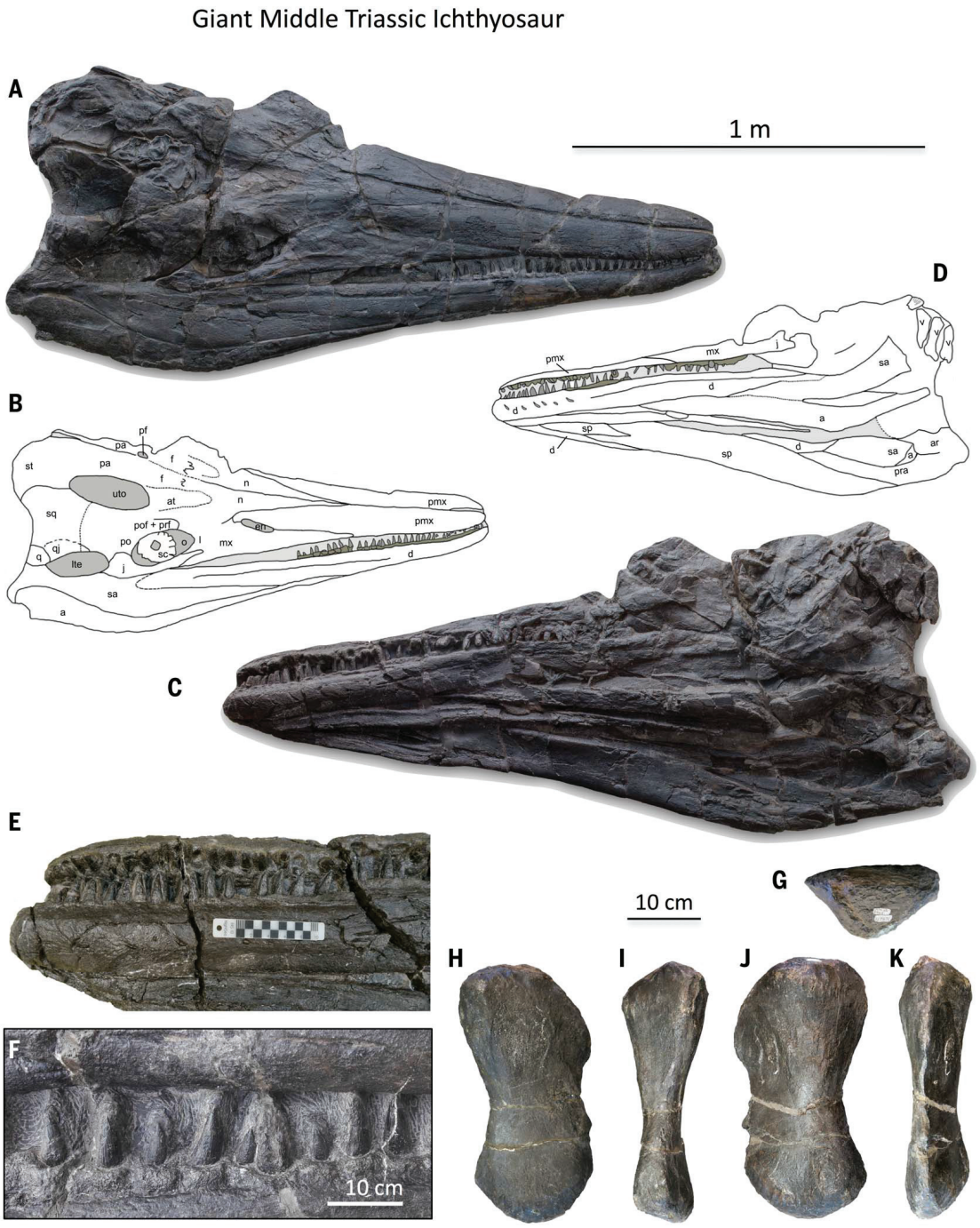

Fig. 2. Skull of the holotype of *C. youngorum* sp. nov. LACM DI 157871. (**A**) Skull in right dorsolateral view. (**B**) Skull sutures. (**C**) Skull in left ventrolateral view. (**D**) Skull sutures. (**E**) Snout in left ventrolateral view. (**F**) Middle part of dentary tooth row in right dorsolateral view. Note the bone of attachment. (**G** to **K**) Right humerus in proximal (G), dorsal (H), posterior (I), ventral (J), and anterior view (K). a, angular; ar, articular; at, anterior terrace; d, dentary; en, external nares; f, frontal; j, jugal; l, lacrimal; lte, lower temporal embayment; mx, maxilla; n, nasal; o, orbita; pa, parietal; pf, parietal foramen; pmx, premaxilla; po, postorbital; pra, prearticular; prf, prefrontal; q, quadrate; qj, quadratojugal; sa, surangular; sc, scleral ring; sq, squamosal; st, supratemporal; uto, upper temporal opening; v, cervical vertebra.

fig. S8A], even though it is available for fewer ichthyosaur taxa than skull length. At 453 mm, the humerus of the holotype of *C. youngorum* sp. nov. is the second largest ichthyosaurian humerus known, translating into a total length of 17.65 m (*10*). The lower 95% prediction interval of its length is 12.48 m; the upper 95% prediction interval is 24.96 m (*10*) (fig. S8A). We also estimated body mass based on a recent dataset for ichthyosaurs (*10*, *24*) (table S5). The regression function (fig. S8B) yielded a body mass estimate of 44,699 kg for the 17.65-m-sized LACM DI 15787 specimen (table S5). The lower mass based on the 95% prediction interval of both regressions is 14,712 kg (lower limit of the 95% prediction interval of body mass against length evaluated for 12.48 m); the upper mass is 135,809 kg (upper limit of the 95% prediction interval of body mass against length evaluated for 24.96 m). These body size metrics of *C. youngorum* sp. nov. result in one of the highest length and mass estimates for any ichthyosaur and the largest taxon of the Middle Triassic: Based on length and scaled-up mass data in Gutarra *et al.* (*24*), *S. popularis* from the late Carnian (about 230 Ma ago) was 13.5 m long and had a mass of 21,651 kg, whereas the middle Norian (about 212 Ma ago) *S. sikanniensis* was 21 m long and had an estimated body mass of 81,497 kg. Taken together, these length and mass estimates place ichthyosaurs in the range of body sizes of living cetaceans, but it appears that ichthyosaurs reached their largest sizes much earlier in clade history than whales.

The fossil record of body-size evolution

Despite the recent interest in ocean gigantism (*4*, *6*, *23*, *24*), detailed comparison of the evolutionary paths to giant body size in cetaceans and ichthyosaurs is lacking so far, as is a phylogenetically comprehensive analysis of

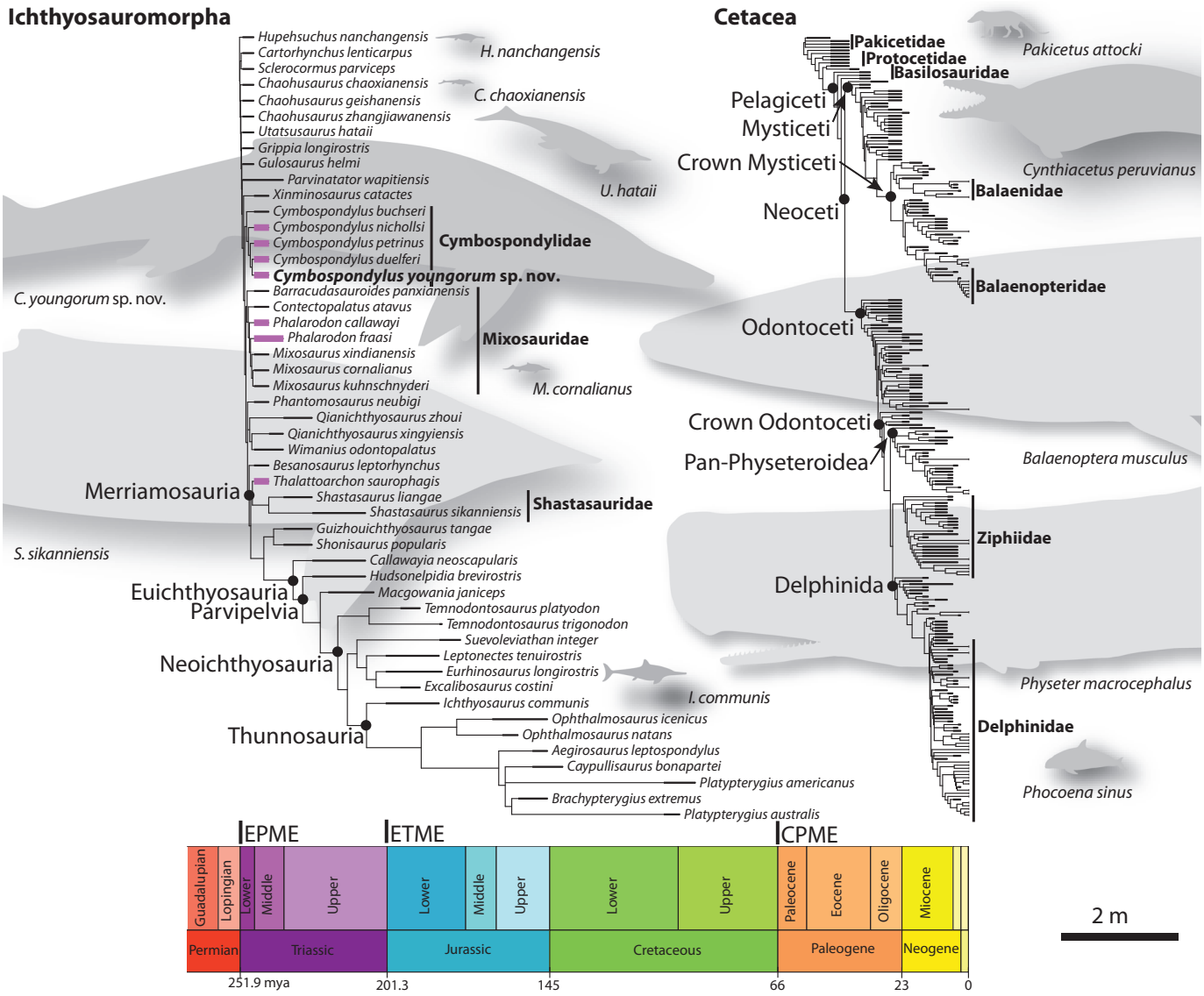

Fig. 3. Time-calibrated phylogenies and body-size illustrations of Ichthyosauria and Cetacea and the relationships of the new giant ichthyosaur *C. youngorum* sp. nov. Ichthyosaurs originated in the late Early Triassic shortly after the end-Permian mass extinction (EPME), survived the end-Triassic mass extinction (ETME), and went extinct in the early Late Cretaceous. Lilac stratigraphic ranges denote taxa from the Fossil Hill Fauna. Cetaceans originated in the late Paleocene after the Cretaceous-Paleogene mass extinction (CPME). See (*10*) for sources of phylogenies and table S6 for image credits. mya, million years ago.

body-size evolution in all Cetacea, including stem taxa (fig. S9). Both ichthyosaurs and cetaceans evolved after mass extinction events (Ichthyosauria after the end-Permian mass extinction event and Cetacea after the Cretaceous-Paleogene mass extinction; Fig. 3), with their respective terrestrial ancestors invading marine ecosystems that differed radically from those that existed before each mass extinction.

The early-branching members of both ichthyosaurs and cetaceans are small compared to later taxa, and both show aquatic adaptations, but to various degrees. The ichthyosaur *Cartorhynchus lenticarpus* from the Early Triassic had a skull length of 55 mm (*7*, *25*), whereas the skull of the cetacean *Pakicetus attocki* from the Eocene reached a width of 127 mm (*10*, *26*). The limbs of *C. lenticarpus* have been interpreted to allow limited terrestrial locomotion, where the cartilage-rich forelimb may have functioned analogously to seal flippers (*25*). The short trunk and snout may have been beneficial for terrestrial locomotion, whereas pachyostotic ribs added to the weight of the animals and perhaps helped with navigating surging water near shores (*25*). *Pakicetus* is interpreted to have inhabited freshwater systems, wading and swimming in shallow water similar to extant hippos, despite its terrestrially adapted limbs (*27*). Upward facing eyes are reminiscent of a crocodilian-like lifestyle at the water surface, enabling vision through air while being submerged in water [analogous to *Tiktaalik* (*28*)]. Increased bone mass through osteosclerosis, stable isotopes, and preferred diet inferred from tooth microwear (*27*, *29*, *30*) further corroborate an aquatic lifestyle.

A literal reading of the geologic time scale implies that body size evolved considerably faster in ichthyosaurs than in cetaceans. Fossils document a rapid size increase in ichthyosaurs from *Cartorhynchus* (55-mm skull length) in the Olenekian at 248.5 Ma ago (*25*) to *C. youngorum* sp. nov. (1890-mm skull length) a mere 2.5 Ma later. Fossils record slower evolution of body size in cetaceans, for example, from *P. attocki* (127-mm skull width) in the late Ypresian (*10*, *26*) to *Basilosaurus isis* (600-mm skull width) in the Priabonian [(*10*) and data S5] 10 to 14 Ma later, and in odontocetes, from *Simocetus rayi* (238-mm skull width) in the Rupelian [(*10*) and data S5] to *Livyathan melvillei* (1970-mm skull width) in the Tortonian [(*10*)

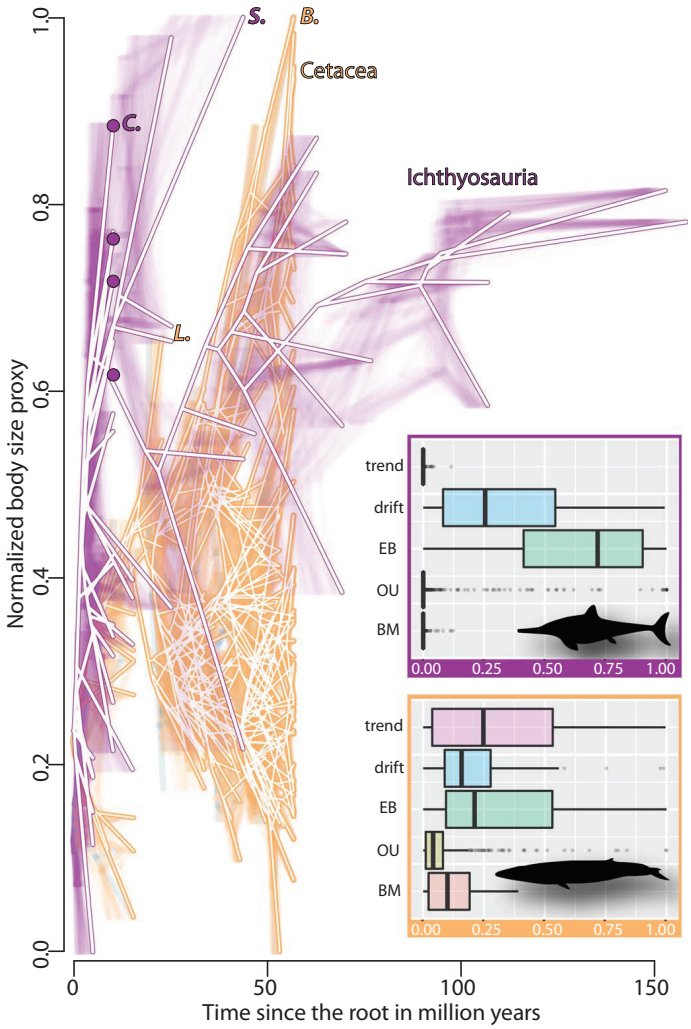

Fig. 4. Body-size evolution in ichthyosaurs and cetaceans compared. Traitgram of body size, normalized such that 0 corresponds to the smallest body size in each group and 1 to the largest for ichthyosaurs (lilac; based on an early-burst model) and cetaceans (ochre; based on a Brownian motion model) (see Methods). Lilac dots indicate *Cymbospondylus* species from the Fossil Hill Fauna. B., *Balaenoptera musculus*, blue whale; C., *C. youngorum* sp. nov.; L., *Llanocetus denticrenatus*, early giant baleen whale; S., *S. sikanniensis*, the largest named ichthyosaur. The inset shows model-fitting results expressed as Akaike weights for five different evolutionary models from 1000 iterations. Boxes represent the interquartile ranges (IQRs), with whiskers extending 1.5 times the IQR outside the boxes. Vertical lines inside the boxes show the median. BM, Brownian motion; EB, early burst; OU, Ornstein-Uhlenbeck.

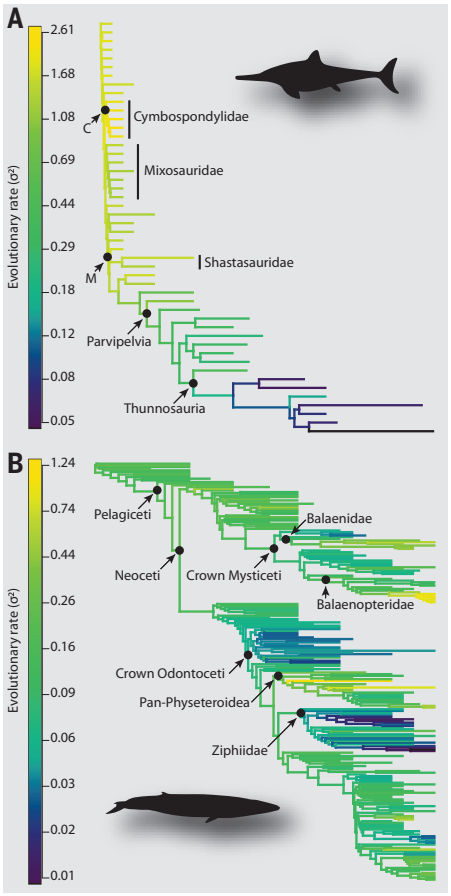

Fig. 5. Exploration of the rate heterogeneity of body-size evolution. (**A** and **B**) Ichthyosaurs (A) feature the fastest rates of body evolution early in their history, whereas cetaceans (B) show a more complex pattern, with fastest rates occurring in later stages of their history. C, Cymbospondylidae; M, Merriamosauria.

and data S5] more than 25 Ma later. These examples illustrate the short time spans of size increases in ichthyosaurs compared with those of cetaceans, but does this pattern hold when analyzed in the context of time-calibrated phylogenies?

Computational modeling of body-size evolution

We first compared the evolutionary patterns of body-size evolution through traitgrams that account for the uncertainty tied to the time calibration of the phylogenies (*10*). These evolutionary traitgrams of ichthyosaur and cetacean body sizes, normalized to maximum body size to enable a better comparison of the pattern, reinforce the notion of fast body-size evolution in ichthyosaurs (Fig. 4). The maximum body size of ichthyosaurs increased dramatically early in their history, whereas cetacean maximum body size increased up to the present day. In our clade-wide model-fitting approaches, the early-burst and trend models are strongly preferred over all other evolutionary models for ichthyosaurs [Fig. 4 and fig. S10; see (*10*)]. By contrast, no strong preference is indicated for any particular model in cetaceans (Fig. 4). Resampling of the cetacean dataset to adjust for differences in sample size, trophic specialization, and the mixture of fossil and extant data did not reveal strong support for an early-burst model (see fig. S11). When restricting the cetacean dataset to the Pelagiceti to account for the differing degrees of aquatic adaptation in the early-branching lineages, an early-burst model is slightly preferred over the others tested (see fig. S11), but the pattern is not nearly as strong as for ichthyosaurs.

To explore the evolutionary patterns at smaller phylogenetic scales and therefore avoid problems related to the impact of taxon selection, we assessed the heterogeneity of the rate of body-size evolution across both the ichthyosaur and cetacean trees (Figs. 5 and 6 and fig. S12). Models that allow for rate heterogeneity can identify specific regions of the tree that signify evolutionary changes and thus circumvent the problem of a clade-wide approach that would ignore the various degrees of aquatic adaptations in the early ichthyosaurs and cetaceans.

Results from a variable-rate model based on Brownian motion, which uses penalized likelihood to estimate the evolutionary rates along all branches in the tree (*31*), support fast evolution of body size in early ichthyosaurs (Fig. 5A). In congruence with observations from the fossil record and clade-wide model fitting, the highest evolutionary rates are found in the

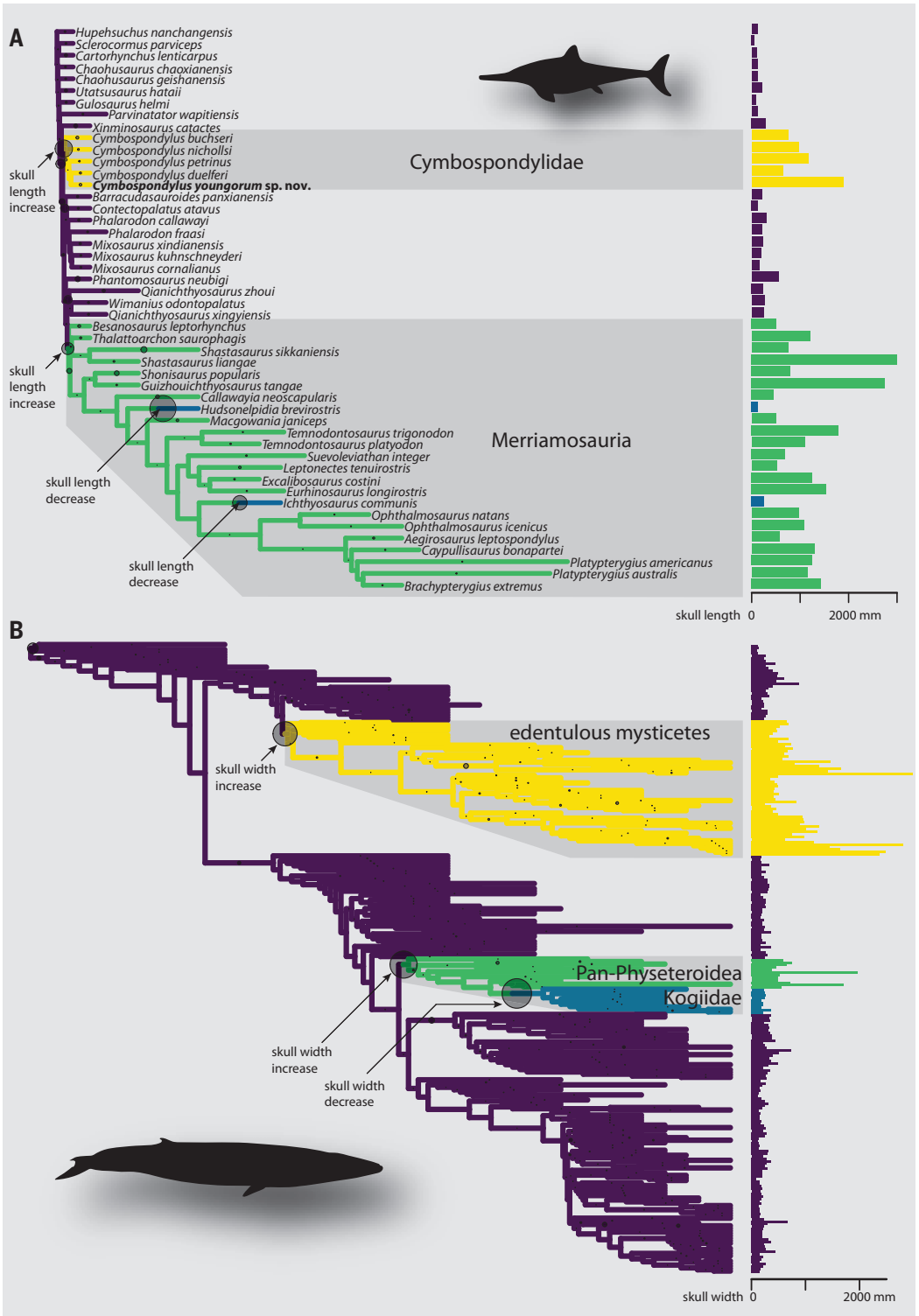

Fig. 6. The adaptive landscape of body-size evolution. (**A** and **B**) Ichthyosaurs (A) feature two early adaptive shifts toward larger skull length, whereas cetaceans (B) entered selective regimes that promoted larger skull width much later in their evolution.

deep regions of the ichthyosaur tree, with some indication that fastest size evolution may have occurred in cymbospondylids and the early phase of merriamosaurs (Fig. 5A). After the initial burst, the estimated evolutionary rates slowed over time.

The distribution of evolutionary rates in the cetacean tree forms a stark contrast to the ichthyosaur pattern (Fig. 5B). The deep parts of the cetacean tree feature average rates. Surprisingly, the body size of both early crown mysticetes and odontocetes evolved slowly, before accelerating in two clades of mysticetes with living representatives, the Balaenidae (right and bowhead whales) and Balaenopteridae (rorquals), as found in a previous study (*6*). Among odontocetes, the fossil lineages of the Pan-Physeteroidea, in particular, a clade that contains living sperm whales, are characterized by fast rates, whereas Ziphiidae (beaked whales) have comparatively slow rates of size evolution (Fig. 5B).

Whereas rate heterogeneity models can identify phases of fast and slow morphological evolution, the determination of the direction of evolution, that is, evolution toward larger and smaller body sizes in specific lineages,

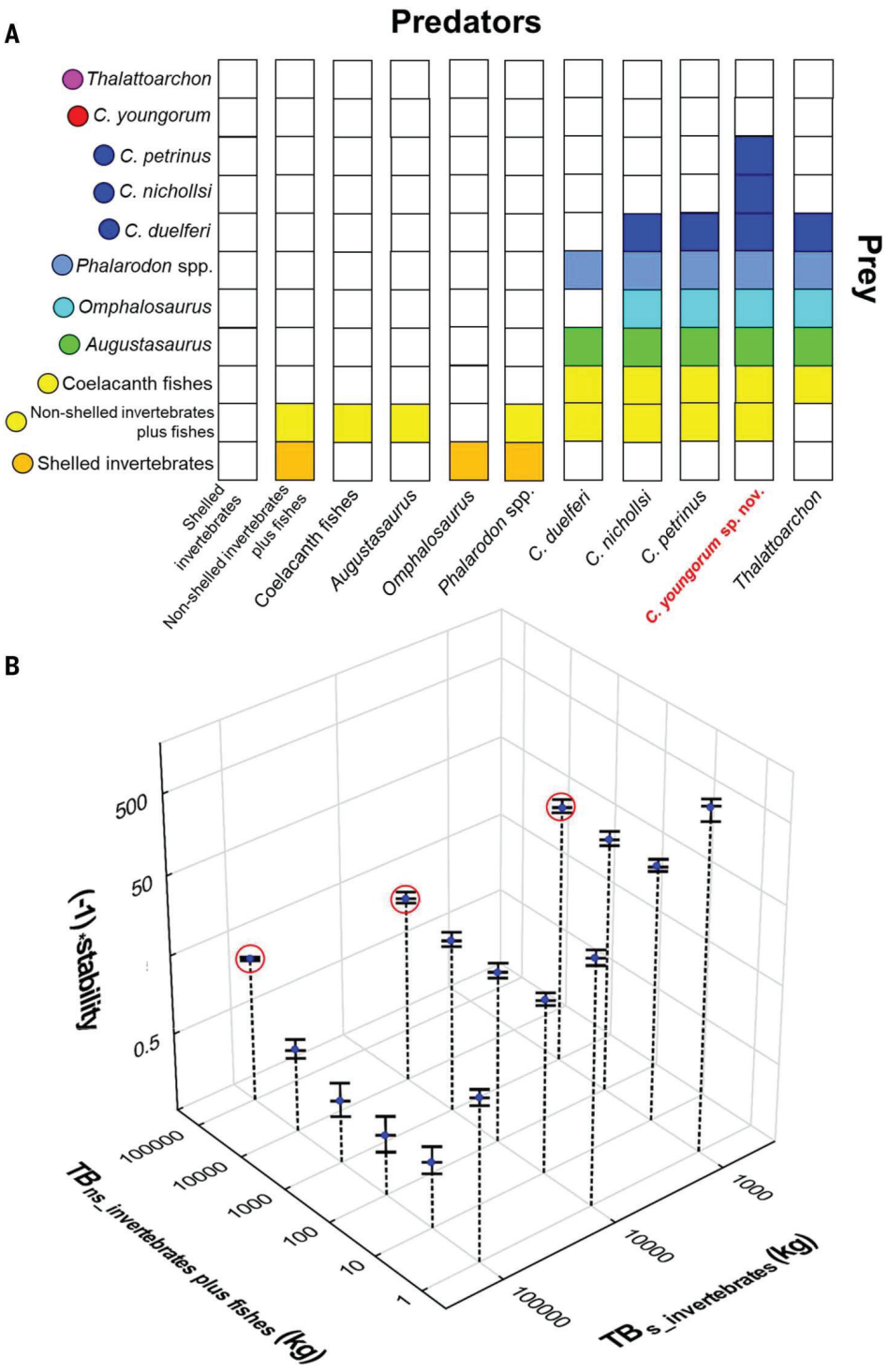

Fig. 7. Energy-flux model and food web stability. We tested whether the food web as preserved is functional and stable over ecological time. All shelled invertebrates (specifically ammonoids), fish, and amniote taxa discovered in the Fossil Hill Fauna are modeled as members of a food web. The member "shelled invertebrates" is basal to the food web and comprises primarily ammonoids but also halobiid bivalves and crustaceans. The member "nonshelled invertebrates plus fishes" ("fish") pools coleoid cephalopods such as squid and small- to medium-sized fish. See Methods and table S11 for food web members and their body masses, total biomasses, and energetic demands. (**A**) Trophic interaction matrix used for modeling energy-flux across members. Stacked bars represent the diet of predatory taxa. Filled squares within bars indicate that a taxon is taken by the predator, whereas white indicates that it is not. (**B**) Stability values calculated by the model for different combinations of total biomass of the two food web members "shelled invertebrates" and "fish." More negative stability values indicate a more stable food web. Error bars for blue dots represent model results assuming maximum and minimum body mass estimates for ichthyosaur taxa (table S11). Greater body masses result in less-stable food webs than smaller body masses. Stability values of extant food webs range between −10 and 0 (*41*). Note that we multiplied stability values by −1 for plotting. TB, total biomass (kg); red circles, the total biomass of "shelled invertebrates" equals that of "fish."

requires complementary approaches. We chose a Bayesian implementation of the Ornstein-Uhlenbeck model of trait evolution (*10*, *32*) to infer whether and when adaptive shifts of body size occurred through evolutionary time and whether smaller or larger body sizes were selected for in the new regime (Fig. 6 and fig. S12). Analyses of the selective regime also enable an evolutionary definition of giants and dwarfs. Adaptive shifts toward larger body size define clades comprising giants, with evidence for selection of larger body sizes, whereas shifts toward smaller body sizes identify dwarfs.

Analyses of the selective regime provide support for two independent shifts toward larger body sizes early in the evolution of ichthyosaurs, defining two clades of giants. One shift toward larger size is reconstructed for the branch leading to the Cymbospondylidae with *C. youngorum* sp. nov., and another shift is placed on the branch leading to the Merriamosauria (Fig. 6A). Both selective regime shifts thus occurred around the boundary between the Early and Middle Triassic. Shifts toward regimes selecting smaller body sizes were inferred for the *Hudsonelpidia brevirostris* and *Ichthyosaurus communis* tip branches (Fig. 6A).

In cetaceans, the geologically oldest shift toward a regime selecting larger body sizes occurred in the late Eocene (Fig. 6B), coinciding with the loss of functional teeth in some lineages of mysticetes (*33*). The Pliocene accelerations of body-size evolution in crown mysticetes are not detected as distinct adaptive

shifts. However, a second shift toward the evolution of large body sizes occurred in the Oligocene, fitted to the branch leading to the Pan-Physeteroidea, which evolved a raptorial feeding mode by the middle Miocene (i.e., *Brygmophyseter shigensis*). An evolutionary reduction of body sizes is inferred for the Kogiidae, a clade nested within the Pan-Physteroidea, with two living species, *Kogia breviceps* and *Kogia sima*, the pygmy and dwarf sperm whales, respectively. Another shift toward smaller body-size evolution may have occurred early in the history of cetacean evolution, in the pakicetids, yet the support for this regime shift is not nearly as strong as the other three identified shifts (Fig. 6B).

Estimates of the phylogenetic half-life [see Methods and (*10*)] suggest that ichthyosaur body size evolved an order of magnitude faster than cetacean body size when entering a new selective regime. Ichthyosaurs thus evolved large body sizes very quickly and very early on in their evolution (Fig. 4 and fig. S10), in oceans thought to be less favorable for large-bodied ecosystem members at higher trophic levels (*9*). Intriguingly, many Cymbospondylidae, which constitute one of the two shifts toward large body sizes, were present in the same assemblage, the Fossil Hill Fauna from the Fossil Hill Member of the Favret and Prida formations of northern Nevada, USA, including *C. youngorum* sp. nov.

The composition of the Fossil Hill Fauna of Nevada

The Favret Formation of the Augusta Mountains (fig. S13), Nevada, USA, spans the middle to late Anisian (Middle Triassic), a period covering more than 2 Ma (*34*). The Fossil Hill Member itself (fig. S13) is a black shale unit of variable thickness deposited in anoxic bottom waters below the storm wave base (*35*). Surface waters were well aerated and must have supported marine reptiles and abundant ammonoids and other invertebrates (*18*, *35*), but there was no benthic life, with the possible exception of halobiid bivalves. The fossils found in the unit thus represent a pelagic ecosystem and food web.

Fish fossils are only rarely preserved (*8*, *10*), but a diverse chondrichthyan fauna (*36*) from just below the Fossil Hill Member suggests that their rarity is due to preservational bias. Comprising eight taxa, the most common marine reptile fossils of the Fossil Hill Fauna are ichthyosaurs (table S10), making it the most speciose ichthyosaur fauna known. Sauropterygia are only represented by a single taxon, the pistosauroid *A. hagdorni* (*8*), in stark contrast to the rich record of sauropterygian fossils from the Tethys Middle Triassic (*37*). Among the ichthyosaurs, *C. youngorum* sp. nov. stands out because of body size, *T. saurophagis* as the oldest apex predator among secondarily aquatic amniotes (*8*), and the holotype of *C. duelferi* (*17*) as the geologically second-oldest gravid ichthyosaur. There are two more large *Cymbospondylus* species (table S3), *C. petrinus* (*38*) and *C. nichollsi* (*16*). Two species of small ichthyosaurs (*Phalarodon fraasi* and *P. callawayi*) differ in the extent of their crushing dentition (*39*). The enigmatic medium-sized *Omphalosaurus* (*40*) is interpreted as a specialized ammonoid feeder (*10*). Notably, filter feeders appear to be absent from the Fossil Hill Fauna.

The enormous size range of marine amniotes in the Fossil Hill Fauna (table S11) rivals the size range seen in modern marine mammal faunas. This range is perplexing given that Middle Triassic oceans lacked the high productivity that is thought to sustain such ecosystems today (*9*). We therefore turned to a new approach in paleontology, energy-flux modeling, to explore whether the Fossil Hill Fauna, as preserved in the fossil record, was a stable food web.

Energy-flux modeling

To test for the stability of the trophic network in the Fossil Hill Fauna, we modeled energy flux with a new tool implemented in R and derived from quantitative ecosystem ecology, "fluxweb" (*41*), which is based on allometric trophic network theory (*42*) and estimates energy fluxes in a top-down approach. In our new implementation for the fossil ecosystem, the model input is preserved taxa and census data and their estimated body masses, energy demands (table S11), and potential prey (Fig. 7A and fig. S14A) (*10*). This tool assesses the food web's stability as the smallest equilibrium total biomass of all modeled food web members by applying a predator-prey multispecies model. Small-shelled invertebrates, including ammonoids, represent the trophically basal member of the food web in the model. The small-shelled invertebrates provide energy directly or indirectly to all trophically higher food web members.

We found that the Fossil Hill food web, with its high phylogenetic diversity and morphological disparity of large to giant endothermic (*10*) ichthyosaurs, was indeed stable (Fig. 7B and fig. S16A). The preserved ammonoids alone provided sufficient energy to the food web as recorded by the fossils (fig. S16C and table S12). Sensitivity analyses demonstrate that the results of the energy-flux model are robust with respect to errors in body mass estimates for ichthyosaurs (figs. S16 and S17) and basal shelled invertebrates (fig. S15) and do not hinge on the assumption of ichthyosaurian endothermy (figs. S15 and S18). Thus, the primary production in the middle to late Anisian was sufficient to support the Fossil Hill food web, including the giant ichthyosaur *C. youngorum* sp. nov. The stability of the Fossil Hill Fauna is also consistent with the lack of pre-Triassic ichthyosaur fossils and the notion that gigantism in ichthyosaurs evolved rapidly in the first few million years of their known history because no hidden Permian history of the clade needs to be invoked (*43*).

The results from our energy-flux model challenge the hypothesis of energetic limitation of maximum body size in Mesozoic food webs (*9*) and provide insights into the functioning of a trophic network without modern primary producers. An important functional characteristic of food webs is the production rate, which is the energy that an individual stores in its body plus the energy that it allocates to reproduction, normally about one-quarter of its basal metabolic rate (*44*). Thus, the sum of the production rates of all individuals in a given trophic level defines the energy that can be transferred to the next level. Our estimates for the production rate of the preserved ammonoid population is congruent with the average production rate of multiple invertebrate species and several modern marine ecosystems (tables S12 and S13). Given that the primary producers of Mesozoic food webs were less productive than their modern equivalents (*9*) and that the trophic level of the largest ichthyosaurs equaled that of the largest living marine carnivores (*8*) and assuming that the energy losses between trophic levels had been the same as those in modern marine ecosystems, the Fossil Hill food web must have had shorter food chains than modern marine food webs.

Although the inferred production rate of all vertebrates in the Fossil Hill Fauna is similar to modern marine ecosystems (table S13), the contributions to this rate by nonamniotes and amniotes differ substantially. The production rates of modern marine amniotes (cetaceans, pinnipeds, birds) are about two magnitudes smaller than the inferred rates for the Fossil Hill Fauna (marine reptiles; table S13), whereas the rates of modern nonamniotes are up to two magnitudes larger than the modeled rates of nonamniotes from the Fossil Hill Fauna (table S13). In comparison to modern marine food webs, the trophic network of the Fossil Hill Fauna was thus dominated by marine amniotes, unlike modern marine food webs that are dominated by nonamniotes. Thus, ichthyosaurs likely occupied niches that are held by fish and whales in modern ecosystems. However, compared with their energetic demands, modeled production rates of the largest ichthyosaur species are small (table S14) and suggest that their densities were lower than suggested by the Fossil Hill Member census.

Comparison of the production rate of preserved ammonites with that modeled for the member "invertebrates" reveals an untapped

energy surplus (fig. S16C and table S12). This surplus may indicate that the food web of the Fossil Hill Fauna as now known is incomplete, perhaps lacking a bulk feeder or other taxa yet to be discovered. Alternatively, the energy surplus actually was untapped in the rather young Fossil Hill food web, being only a few million years old, and consumers of the surplus might have been added in the course of evolution later. Our energy-flux modeling indeed shows that the food web could have supported another giant marine amniote, if it fed in bulk low in the food chain (fig. S19), for example, by filter feeding (*4*). This mode of life possibly arose later in ichthyosaurs, as suggested by the existence of some Late Triassic giant toothless ichthyosaurs (*45*). Filter feeding is important in modern marine vertebrates, for example, baleen whales, the whale shark *Rhincodon typus*, and the basking shark *Cetorhinus maximus* (*46*). Even with a giant bulk feeder, the estimated energy flux from the trophic group comprising the shelled invertebrates passed on to higher trophic levels is still smaller than the estimated amount of energy provided by the preserved ammonoids (figs. S20 and S21 and table S13). Whereas there is no fossil evidence for a filter-feeding ichthyosaur in the Fossil Hill Fauna yet, the results of the energy-flux model demonstrate that this fauna was not only stable but, with its abundant ammonoids and short, amniote-dominated food chains, also set the environmental stage that led to the evolution of large body sizes early on in the evolution of ichthyosaurs.

Implications for body-size evolution of marine amniotes

The appearance of marine amniotes in the Triassic followed on the heels of amelioration of environmental conditions in the first 2 Ma of the Triassic together with a general recovery of marine ecosystems (*47*, *48*). At an estimated body mass of more than 40 tonnes and a geologic age of 246 Ma, *C. youngorum* sp. nov. was a giant marine amniote, attaining a body size comparable to that of today's ocean giants. This new giant may even have approached the size of today's largest cetacean *Balaenoptera musculus* (total length: mode of 25 m) [dataset in (*46*)], given that the Fossil Hill energy-flux model remained stable when we performed the analysis with the upper limit of the body-mass estimate of *C. youngorum* sp. nov. (24.96 m, 135,809 kg). On land, equivalent body masses did not evolve until >40 Ma later, among sauropod dinosaurs of the Jurassic. Apparently, the pelagic environment may be more conducive to the evolution of giant tetrapods. Alternatively, ecosystem recovery from the end-Permian extinction was much slower on land than in the sea. In the sea, only other ichthyosaurs in the Late Triassic and cetaceans since the late Paleogene (38 Ma ago) reached this body size again. The discovery of a giant ichthyosaur so early in the phylogenetic history of the clade underscores the existence of major selective advantages of large body size (*49*).

The Fossil Hill Fauna records a surprisingly diverse and morphologically disparate fauna of large-bodied to giant ichthyosaurs shortly after the end-Permian mass extinction. Unlike the contemporaneous faunas from the western Tethys and China, which are representative of shallow seas on continental shelves, shallow basins, and lagoons (*50*), the Fossil Hill Fauna provides a glimpse into the pelagic habitats of the Middle Triassic. We propose that ichthyosaurs initially benefited from the rapid recovery of conodonts (*51*) and pelagic ammonoid cephalopods (*47*), permitting giant body size soon after oceanic geochemical conditions had stabilized in the Middle Triassic (*48*). Ichthyosaurs may have been able to increase the total amount of resources available to them by virtue of their large eyes (*52*). Large eyes improve the range from which prey can be detected in the clear water of the pelagic realm, both in well-illuminated water near the surface and at greater depth (*53*). Proportionately large eyes seem to have evolved very early in the evolutionary history of the group (*52*), possibly enabling ichthyosaurs to better exploit their food resources. Their energetically costly endothermy could have increased their foraging capacity (speed and success) and energy intake in cold-water habitats, as found in colder geographic regions or in deeper waters (*54*). Mesothermy, which enabled body temperatures intermediate to those of ecto- and endotherms, was important in the evolution of elasmobranch gigantism (*55*).

We have identified two major evolutionary pathways to large body size in cetaceans. Size evolution in odontocetes may be linked to the evolution of raptorial feeding mode in some taxa and deep diving in others (*4*, *56*). Raptorial feeding is one of the drivers for the independent evolution of large body sizes in different clades. This is further evidenced by the earliest inferred raptorial feeder, *Ankylorhiza tiedemani*, which is considered to be the largest Oligocene odontocete with an estimated body length of 4.8 m (*57*), and in the extant delphinid *O. orca*. The evolution of echolocation, which allowed odontocetes to forage at greater depths in search of cephalopods unavailable to early cetaceans lacking a biosonar, is not directly coupled with evolution of size. Biosonar evolved more than 14 Ma before our reconstructed shift toward larger body sizes in the pan-physesteroids (*58*). In mysticetes, the initial shift toward large body sizes coincides with a loss of functional teeth in some lineages of mysticetes and presumably a switch of diet preference. In addition to evolving bulk-feeding adaptations, gigantism in mysticetes appears to be driven by global oceanic changes, particularly over the past few million years, which affected prey distribution and density (*6*, *59*). *C. youngorum* sp. nov. thus demonstrates that the lack of carbon sinks and modern primary producers is not a prerequisite for gigantism [contra (*9*)], challenging the notion that changes in ocean productivity and ecological escalation are necessary preconditions for the evolution of giant body size. Although both cetaceans and ichthyosaurs evolved very large body sizes, their respective evolutionary trajectories toward gigantism were different.

Methods

Phylogenetic analysis of ichthyosaurs

We scored the holotype specimen of *C. youngorum* sp. nov. (LACM DI 157871) into the character matrix of (*17*). This matrix (*17*) had been modified from other recent work (*7*, *60*) and appeals because the character descriptions are drawn from many different sources. We could score 40% of the 287 characters in the matrix with confidence for the new taxon (data S1) but note that many characters in this list were initially defined for post-Triassic ichthyosaurs. We edited the character-taxon matrix with Mesquite v. 3.02 (*61*). Our primary analysis (analysis I; Fig. 3 and fig. S7) included the taxon set of (*17*) with *C. youngorum* sp. nov. added (totaling 60 taxa) and was performed with TNT (*62*) using both "new technology" (search parameters: xmu=hit 20 drift 10) and "traditional" searches. See table S4 for statistics of this and the following analyses. To test for the influence of taxon sampling on the phylogenetic relationships, we used a reduced taxon set with a focus on Triassic ichthyosaurs (analysis II). This reduced taxon set is equivalent to the list of taxa used in (*63*) with the addition of *C. duelferi* and *C. youngorum* sp. nov. Note that we did not use the taxon-character matrix of (*63*), only the same taxa (data S2). A further modification was that we included three representative parvipelvians (*H. brevirostris*, *I. communis*, and *Stenopterygius quadriscissus*), instead of a clade Parvipelvia as in (*63*), to represent this derived clade (analysis III). Finally, we analyzed this matrix with PAUP* 4.1b (*64*) on a Mac computer (analysis IV). Using the heuristic search algorithm and 1000 replicates, 308 most parsimonious trees (MPTs) of 843 steps in length were retained (table S4). The strict consensus was poorly resolved, but the 50% majority rule consensus of these 308 trees shows the same topology as that found by TNT using the same matrix.

The major difference between the four analyses is in the placement of the *Cymbospondylus* clade. The analyses of the modified Klein *et al.* (*17*) taxon set (analyses I and II) recover the clade as earlier branching than, or in a trichotomy with, mixosaurids. The TNT analyses of the

modified Huang *et al.* (*63*) taxon set (analysis III) finds *Cymbospondylus* as later branching than mixosaurids and the Carnian *Toretocnemus*, *Qianichthyosaurus*, and *Californosaurus*. The PAUP analysis (analysis IV) finds the genus as later branching than the Carnian *Toretocnemus* and in an unresolved trichotomy with the Carnian *Qianichthyosaurus* and *Californosaurus*. Because the first analysis (analysis I) is the most conservative in showing the greatest similarity with recently published analyses of Triassic ichthyosaurs (*17*, *63*) and has a fully resolved strict consensus and a low number of MPTs (table S4), we consider analysis I to be our preferred hypothesis (data S3).

Total length estimate for LACM DI 157871

Of the commonly used body-size proxies—total length, skull length, humerus length, and body mass—only two, skull length and humerus length, can be directly measured in LACM DI 157871 and the other two must be estimated. We estimated the total body length of LACM DI 15787 from its humerus length after having conducted a revised regression analysis on a published dataset for Triassic ichthyosaurs (*23*) (fig. S8A and table S5). Contrary to Scheyer *et al.* (*23*), we log10-transformed total body length and humerus length before linear regression analysis, related body length to humerus length, and calculated 95% prediction intervals around the regression line (fig. S8A). This regression analysis was conducted in the software R, version 3.5.2 (*65*).

Body-mass estimates for the Fossil Hill Fauna ichthyosaurs

To estimate body mass of *C. youngorum* sp. nov. (as represented by LACM DI 15787) and the other ichthyosaur species in the Fossil Hill Fauna from total length, we generated a new dataset of body masses for Triassic ichthyosaurs (table S5) for a regression analysis of body mass on total body length (fig. S8B). This new dataset is based on a published compilation of the total body lengths of selected ichthyosaur fossil specimens (*24*). This publication further provides species-specific reference body masses for 1-m-long digital models of these fossils. To estimate body mass for each of the ichthyosaurs in the dataset (table S5), we used the respective reference mass (*24*) for each and up- or down-scaled its body mass to total body length. Note that we excluded the Jurassic ichthyosaurs from consideration because of their different body shape. After having log10-transformed total body length and body mass data from table S4, we carried out a linear regression analysis (fig. S8B) that again includes 95% prediction intervals. This regression analysis was conducted in the software R, version 3.5.2 (*65*).

Phylogenetic hypothesis for cetaceans

To look into body-size evolution in cetaceans, we compiled a comprehensive phylogeny with a special focus on early whales. This phylogeny (fig. S9) includes 250 taxa from the earliest cetaceans to representative extant species. Most large morphological or combined phylogenetic analyses of cetaceans derive from the character state matrix first published by Geisler and Sanders (*66*), with modifications made in subsequent works (*10*). However, taxon sampling in those large data matrices tends to fall short for specific groups (e.g., Ziphiidae, Pan-Physeteroidea). To have a more complete taxon sampling represented in our tree, we used the results of morphological analyses using character state matrices with less taxa, but with a more thorough sampling for specific groups, for example, for Pan-Physeteroidea (*10*). Our phylogeny is thus a combination of the results of several analyses using a variety of different morphological matrices. Although taxon sampling sometimes varies among these works, the relationships between different cetacean groups are generally stable and consistent.

The topology of our composite phylogeny agrees well with a new, comprehensive phylogenetic hypothesis presented in a recent study (*67*) regarding the position and relationships of major clades, only differing in a few minor regards. The first is that our taxon sampling is smaller, in large part because we prioritized the inclusion of species for which proxy data for body size (i.e., bizygomatic width or orbital and postorbital width) were available. Because of this requirement, we did not include *Himalayacetus subathuensis*, which is considered as the earliest cetacean, because the specimen consists of an incomplete mandible (*68*) and instead chose *P. attocki* as our earliest cetacean, which is known from more complete cranial material (*26*). The topology of Lloyd and Slater (*67*) differs from ours by having a polytomy amongst some of the more basal mysticetes (i.e., *Llanocetus denticrenatus*, *Mystacodon selenensis*). Our topology differs in the more inclusive definition of Aetiocetidae that includes *Borealodon osedax* and *Aetiocetus* (*Niparajacetus*) palmadentis, following (*69*). Concerning the odontocete section of the phylogeny, we are using a more inclusive Platanistoidea and Kentriodontidae (*70*, *71*). These differences largely derive from the analyses we used to construct our phylogeny but do not affect our results.

Time calibration of phylogenies

We used stratigraphic ranges at the stage level to time-calibrate the phylogenies (*10*). First and last appearance dates of taxa were defined as the beginning and end of each geologic stage in which the tip taxon is found (data S4 and S5). The geologic age in million years for each stage was taken from Walker *et al.* (*34*). The time calibration of the trees was performed using the R package "paleotree" (*10*) (data S6). Given that the stratigraphic occurrence of many ichthyosaurs and fossil cetaceans is not well defined, we used the most simplistic a posteriori dating approach, implemented in the "timePaleoPhy" function of "paleotree." The initial root ages were set to 251.9 and 56 Ma ago for ichthyosaurs and cetaceans, respectively. We generated sets of time-calibrated trees with the "equal" method (*10*) combined with the "minMax" option. Polytomies were resolved randomly, and for each random resolution, an internal branch length of 1 Ma was added to the tree. This is an arbitrary but, we think, reasonable estimate given the overall tree height of the clades we were working with. For plotting (Fig. 4) and applying methods that allow heterogeneity of parameters across the tree, we also generated trees with the "firstLast" setting, with terminal edges added. The "firstLast" option treats the stratigraphic bins as hard constraints. Trees shown in Fig. 4 were time calibrated with the "DatePhylo" function of the R package "strap" (*10*), also using the "equal" method, and then plotted against the geologic time scale with the "geoscalePhylo" function. The resulting time-calibrated trees for ichthyosaurs agree well with previously published phylogenies for the group, and our cetacean tree generally agrees with those of McGowen *et al.* (*72*) and Lloyd and Slater (*67*). Our divergence estimates for major clades are sometimes a few million years older (e.g., Balaenidae), younger (e.g., Balaenopteridae), or nearly identical (e.g., Pan-Physeteroidea). Such discrepancies likely reflect differences in taxon sampling and time-binning methods (*10*).

Computational analysis of body-size evolution summary

We chose skull-related metrics because skull width (bizygomatic width) is an established size proxy in cetaceans [e.g., (*73*)], as is skull length in ichthyosaurs (*7*). We used the latter dataset for ichthyosaurs, including some additional data from the recent literature and this study (data S4). Specifically, we added the skull length of two more species of *Chaohusaurus*, *C. chaoxianensis* and *C. zhangjiawanensis*, among Early Triassic taxa. Note that the specimen of *C. chaoxianensis* that provides the skull length has recently been assigned to a new species, *C. brevifemoralis*, sister taxon to *C. chaoxianensis* (data S4). Among Middle Triassic taxa, we added the specimen described in this study and the recently described *C. duelferi* from the same beds (*17*) to the dataset. The dataset of cetacean bizygomatic width relies on many sources and includes a number of new data points (data S5).

We first evaluated the fit of trait evolution models to the data for the given phylogenies

(fig. S10) with a maximum likelihood approach, using the "fitContinuous" function of the R package "geiger" (*10*) (data S6). We fit five different models with macroevolutionary relevance [(*10*) and table S7]. We ran the primary analyses over 1000 trees with slightly differing time calibration and the subsequent resampling analyses to explore the data in more depth over 100 different trees. For each iteration, we normalized branch lengths to avoid computational problems. We evaluated model fit by means of the sample-size corrected Akaike information criterion (AICc) and their corresponding Akaike weights over the entire tree sets. Akaike weights are useful because they represent the conditional probability for each of the tested models (*10*). To account for any artifactual or other nonbiological differences between our ichthyosaur and cetacean datasets, we not only performed model fitting for the entire dataset but also carried out several resampling approaches of the cetacean data. Altogether, we completed nine different model-fitting approaches (see fig. S11).

To illustrate the patterns of body-size evolution in ichthyosaurs and cetaceans, we selected a new modification of the well-established evolutionary traitgram approach (*10*). In evolutionary traitgrams, the phylogeny is combined with ancestral state reconstructions for the nodes through a projection of the tree into a space defined by the trait value on the y axis and time on the x axis (or sometimes vice versa). We intended to achieve a direct comparison of ichthyosaur and cetacean body-size evolution in the same diagram. To realize this type of visualization, we had to overcome several hurdles. First, we used different size proxies for ichthyosaurs (skull length) and cetaceans (skull width), and thus the trait values are not directly comparable in visual terms. To solve this issue, we normalized the trait values so that the smallest and largest trait values for both ichthyosaurs and cetaceans ranged from 0 to 1, respectively (Fig. 4). Second, ichthyosaurs and cetaceans originated at different times in geologic history. To facilitate their direct comparison, we started each traitgram at the root of the tree (Fig. 4), irrespective of absolute geologic time. Third, the mode of body-size evolution differs between ichthyosaurs and cetaceans, with early burst–like processes dominating ichthyosaurs and no clear pattern for the full cetacean dataset. We therefore reconstructed the traitgrams for cetaceans with the simplest evolutionary model (Brownian motion) and for ichthyosaurs using an early-burst model (fig. S10). Finally, to illustrate uncertainty stemming from the difficulties of proper time calibration, we devised and applied a new approach for traitgram plotting. The stratigraphic ranges of many extinct taxa are not well defined, and as such, the branch lengths of our trees are uncertain. To take this uncertainty into account, we plotted a range of different possible evolutionary traitgrams into the same diagram, using semitransparent colors (Fig. 4 and fig. S10). Dense, more opaque areas in the traitgram space therefore indicate evolutionary time and trait combinations with a high probability of containing the true evolutionary path of body size, whereas empty areas are less probable (Fig. 4 and fig. S10). For both ichthyosaurs and cetaceans, we also added the traitgrams that one would expect if the last appearance date were taken at face value, that is, if all taxa existed to the very end of the stage they have been documented for. These traitgrams are in white color. The evolutionary traitgram approach was implemented using the R package "phytools" (*31*) (data S6).

To identify regions of the tree with accelerated phases of evolution, we explored heterogeneity in the rate of trait evolution across the phylogeny using the function "multirateBM" of the R package "phytools" (*10*, *31*). This method is based on a penalized likelihood in which we fit a multirate Brownian motion trait evolution model in which the rate (σ^2) evolves by a correlated random-walk process. Every edge of the tree is consequently allowed to have a slightly different value of σ^2. The penalty term, which is based on the probability density of the evolutionary rates σ^2 along all branches in the tree multiplied by a user-specified coefficient denominated λ, is necessary to identify both the evolutionary rates along all the edges of the tree, as well as the rate of Brownian evolution of the rate itself. Low values for the penalty coefficient λ (e.g., 0.01) will tend to accord very little penalty to rate variation among edges, whereas higher values (e.g., λ = 100) permit the rate to differ little. Intermediate λ values (e.g., 1) balance the probability of the data under the model and the probability of the rate variation among edges, given a Brownian evolution process for rate variation. We set λ = 0.1 for both ichthyosaur and cetacean datasets and verified that the overall pattern remains consistent for $0.01 \leq \lambda \leq 1$. Given that we did not perform a full cross-validation of λ, we consider the results exploratory.

The second approach to assess body-size evolution along the edges of the phylogeny is founded on a Bayesian implementation of the Ornstein-Uhlenbeck method [R package "bayOU" (*32*)]. The Ornstein-Uhlenbeck model of trait evolution is an extension of the Brownian motion model and describes a random walk coupled with the tendency of trait values to stay in proximity of a stationary peak (θ). The tendency of the trait to remain close to the peak is measured by the parameter α, which is interpreted as the strength of selection. BayOU analyses thus characterize the selective regime of a trait.

BayOU agnostically infers whether adaptive shifts of the peak θ occurred through evolutionary time and, if so, along which edge in the phylogeny these changes likely happened. Bayesian approaches to such inferences are also less prone to error for small phylogenetic comparative datasets (N < 100) than other methods (*74*), which is useful for the ichthyosaur data. Probabilistic prior settings are summarized in table S8.

The reversible jump Markov chain Monte Carlo simulations were run for 3 million generations for the ichthyosaur data and 6 million generations for the cetacean data, of which the first 30% was discarded as burn-in. We ensured that independent chains had converged on similar regions in the parameter space by Gelman's R for log likelihood, σ^2, and α (fig. S12 and table S9). We also checked for convergence by plotting the posterior probabilities for shifts along branches against each other. If convergence was achieved, the posterior probabilities should fall along a line with a slope of 1 (fig. S12). We considered an adaptive shift well-supported if its respective posterior probability was far outside the main distribution of posterior probabilities for all branches.

Among ichthyosaurs, four branches with mean posterior probabilities of 0.41 to 0.86 [39 to 81 times greater than their prior probability (0.01)] were chosen (see table S8). The mean estimate of α is 0.4, indicating a phylogenetic half-life [$\ln(2)/\alpha$] of 1.73 Ma. Applied to cymbospondylids, the ichthyosaurs in this clade evolved halfway from their previous adaptive peak of 135 mm to their new peak (1443 mm) in 1.73 Ma, which is congruent with the fossil record. The phylogenetic half-life of cetacean skull width is 17.3 Ma. Among cetaceans, three branches with mean posterior probabilities of 0.84 to 0.95 [413 to 472 times greater than their prior probability (0.002)] were chosen (see table S8). Another branch received a posterior probability of 0.36, far less than the other three shifts and not as clearly separated from the distribution of posterior probabilities. If supported, this adaptive shift would suggest that the Pakicetidae shifted toward smaller body size, with a new peak 62-mm skull width as opposed to the ancestral state estimate of 121 mm. Other interesting patterns are apparent in cetacean size evolution, such as the missing middle size classes in the Oligocene and repeated increases of body-size ranges in different clades, but fully exploring them is beyond the scope of this study.

Energy-flux modeling summary

To test whether the composition of the pelagic Fossil Hill Fauna as found in the fossil record (fig. S13 and table S10) represents a functional and stable food web (hypothesis 1, standard scenario), we modeled energy flux using a

new tool from quantitative ecosystem ecology implemented in R, "fluxweb" (*41*), which is based on allometric trophic network theory (*42*). Importantly, it derives energy fluxes in a top-down approach. The "fluxweb" tool calculates the food web's stability (*41*) by applying a predator-prey multispecies model and searching for equilibrium total biomasses of food web members. More negative stability values indicate a more stable food web, that is, the smallest equilibrium total biomass across all food web members is larger than zero, whereas a positive stability value indicates that at least one food web member is extinct under equilibrium.

Model input is census data of preserved taxa (all of which are pelagic) as members of the food web, estimated body masses, energetic demands (table S11), and potential prey (Fig. 7A and fig. S14). For modeling, we added two further members that are lowest in the food web and pool different kinds of animal taxa. We pooled taxa because we lack sufficient information on the parameter values required for modeling each taxon individually, and we aimed to keep our model as simple as possible. The first additional member is "shelled invertebrates" ("invertebrates" for short). This member is basal in the modeled food web and comprises primarily ammonoids but also halobiid bivalves and crustaceans. It pools the trophically lowest invertebrates of the Fossil Hill Fauna preserved in the fossil record. The "invertebrates" directly or indirectly provide energy to all other members of the food web. How this energy is produced in a basal member is ignored in "fluxweb" (*41*), and thus modeling of predator-prey relations within basal food web members is not possible in this tool. The second additional member is "pooled nonshelled invertebrates and fish" ("fish" for short). This member pools coleoid cephalopods such as squid and small- to medium-sized fish. It thus comprises the preserved and unpreserved taxa of the lowest trophic level on which the majority of all other trophically higher members fed (Fig. 7A and fig. S14). For the member "fish," we implemented potential within-group predator-prey relations by allowing that "fish" feed on "fish" (Fig. 7A and fig. S14) because larger fish could potentially have fed on smaller fish and squid. We further assume in our model that energy demands of all ichthyosaur taxa equaled that of modern endothermic vertebrates (*10*), whereas demands of all other taxa either equaled that of ectothermic vertebrates or of ectothermic invertebrates.

For the two members "invertebrates" and "fish," we evaluated our model for 15 different combinations of total biomasses because we lack reliable information on their total biomasses from the fossil record. Because the body masses estimated for the ichthyosaur taxa used in our model and total biomasses derived from these all have large margins of error and because the ichthyosaurs are the largest animals of the Fossil Hill Fauna, we evaluated each of the 15 combinations for standard body mass, lower limit of body mass, and upper limit of body mass based on 95% prediction intervals (table S11). A sensitivity analysis of body mass of basal "invertebrates," for which the fossil record documents a body mass variation of about five orders of magnitude, showed that potential errors had an extremely small impact on stability values and energy fluxes calculated by our model (see below and fig. S15). In the three combinations, in which the total biomass of "invertebrates" equaled that of "fish," the average energy loss between two trophic levels always turned out to be the highest across the 15 combinations, and estimated losses of around 40% were clearly unrealistic from a modern perspective (figs. S16B and S19, B and F). We thus restricted our ecological and evolutionary interpretation of modeling results to the other 12 combinations in which the total biomass of the "invertebrates" was larger than that of the "fish."

Although we assumed that energy demands of all ichthyosaurs in the Fossil Hill Fauna conformed to modern endotherms [table S11 and (*10*)], we nevertheless wanted to test model sensitivity to this assumption. We thus reran the model for all combinations assuming ectothermic and mesothermic (*54*) ichthyosaurs. Endothermy in any of the taxa in the model (table S11) results in a higher energy consumption than ectothermy and mesothermy (fig. S15). We considered mesothermy as a metabolic strategy for ichthyosaurs because several modern marine macropredators show this strategy—for example, tunas, swordfish, and lamnid sharks (*54*)—and because mesothermy was important in the evolution of elasmobranch gigantism (*55*).

The "fluxweb" tool provides different allometric equations on mass-specific metabolic rates for implementing different energetic demands (i.e., physiological losses; fig. S15). The ectothermic and the endothermic vertebrate metabolic types of "fluxweb" only differ in their use of scaling normalization constants: 19.5 for the endothermic metabolic type versus 18.18 for the ectothermic metabolic type (table S11). To implement mesothermy, we used the arithmetic mean of the two, 18.84. The scaling exponent of all three metabolic types is −0.29 (table S11). To assess the effect of the ectothermic and mesothermic metabolic types on stability values and energy fluxes, we reran the model for mesothermic and ectothermic ichthyosaurs while keeping everything else as in the standard scenario (fig. S18).

To narrow down which total biomass of the basal "invertebrates" are the most realistic for the food web of the Fossil Hill Fauna, we estimated the total biomass of ammonoids found in the Fossil Hill Member of the Augusta Mountains from field data (table S12). We are aware of the limitations of this approach because ammonoids usually accumulate in certain layers, are not evenly distributed throughout the Fossil Hill Member, and comprise different species. To estimate total ammonoid biomass, we conducted a census by shell diameter on one randomly chosen surface of 1 m^2. Recognizing five size classes, we found the following abundances: I, >23 cm diameter, one individual; II, 23 to 6 cm, 28 individuals; III, 6 to 3 cm, 49 individuals; IV, 3 to 1 cm, 49 individuals; and V, <0.5 cm, 28 individuals. To estimate the biomass of these individuals, we used an extant *Nautilus belauensis* with a 23-cm shell diameter and a mass of 1.675 kg (*75*) as a proxy and linearly downscaled its size and mass to estimate the weight of the smaller ammonoid individuals. This calculation and census of a total of 155 individuals yielded an average body mass of about 10 g. This is the rounded mean calculated from frequencies of individuals in size classes and body masses corresponding to the respective lower-size class boundaries (except for class V, for which we used a 0.5-cm shell diameter). The abundances and body masses of the five size classes further yielded about 2.7 kg as an estimate of ammonoid biomass per square meter. A field census of random samples in the Augusta Mountains suggested that 15% (0.540 km^2), 25% (0.900 km^2), or 30% (1.080 km^2) of the Fossil Hill outcrop area (3.6 km^2) is covered by ammonoids, which corresponds to a total biomass in this area of 1458 kg, 2430 kg, or 2916 kg, respectively. We used the estimated average ammonoid body mass (10 g) for the member "invertebrates" in the "fluxweb" model (table S11).

To assess a potential impact of the body mass assumed for "invertebrates," we evaluated the model with a body mass of "invertebrates" of 0.02 g (size class V) and of 1.675 kg (size class I) for the standard scenario. Our rationale was that this member provides the energy to all other trophically higher members and that their body-mass range documented in the fossil record covers nearly five orders of magnitude. However, for both body masses, the stability values and energy fluxes obtained were nearly identical to those obtained for the standard mass of 10 g. With respect to this observation, it is important that the body mass assumed for any modeled food web member (i) is used to calculate its physiological losses (model parameter X_i). Except for "invertebrates" and "fish," body masses of all members were also used to calculate their total biomasses as a product of body mass and number of counted individuals (table S11). Because the total biomass of "invertebrates" and "fish" is fixed in each model run, only physiological losses are

altered by changing body masses. An evaluation of the equations used for physiological losses shows that whereas the body-mass range covered by the food web members spans about 10 orders of magnitude (the mass corresponding to the smallest ammonite size class V is 0.02 g, and the upper body mass limit of *C. youngorum* sp. nov. is 135.81 tonnes), the variation in losses is smaller than one magnitude over this huge range (fig. S15). For the members "fish," coelacanth fish, and *A. hagdorni*, we estimated body masses from related and similar taxa because we lack any information about their body mass and its variation in the Fossil Hill Fauna. We therefore refrained from carrying out a sensitivity analysis for body mass for these three members. Based on the arguments given above, modeling results must also be very insensitive to the body mass assumed for the members "fish" and coelacanth fish. There is only one coelacanth fish individual in the Fossil Hill Fauna, and thus its total biomass equals its body mass (table S11). However, the census for *A. hagdorni* is three individuals, and any change in the body mass assumed for this member results in a change in its total biomass. Thus, we cannot exclude the possibility that this change will alter stability values and energy fluxes. We anticipate that these values will be in the range found for ichthyosaur members with a similar body mass and total biomass.

Modeling the Fossil Hill Fauna with a hypothetical giant bulk feeder

Averaged across the 12 combinations of total biomasses of "invertebrates" and "fish," the production rate of "invertebrates" was a magnitude smaller than that of the preserved ammonoids (fig. S16C and table S12). We thus conducted a second modeling experiment (hypothesis 2) in which we added a hypothetical blue whale–sized endothermic ichthyosaur (200 tonnes, about 30 m long) to the Fossil Hill food web model while keeping everything else as in the standard scenario. This super giant bulk feeder exclusively fed on either "invertebrates" (fig. S14B) or "fish" (fig. S14C). For both feeding strategies, the hypothesized food web was again stable (fig. S19A), and for each chosen combination of total biomass of "invertebrates" and "fish," food web stability was somewhat higher than in the standard scenario (fig. S20A). When averaged across the possible combinations of total biomasses of "invertebrates" and "fish," the supergiant that fed exclusively on "invertebrates" consumed an increase in outgoing energy from "invertebrates" of 2.6×10^{-7} kJ/year and the supergiant that fed exclusively on "fish" consumed 1.7×10^{7} kJ/year (fig. S21). A detailed description of our model, a justification of model assumptions, and output variables inferred is in the supplementary materials (*10*).

REFERENCES AND NOTES

1. G. J. Vermeij, Gigantism and its implications for the history of life. *PLOS ONE* **11**, e0146092 (2016). doi: 10.1371/journal.pone.0146092; pmid: 26771527
2. N. P. Kelley, N. D. Pyenson, Vertebrate evolution. Evolutionary innovation and ecology in marine tetrapods from the Triassic to the Anthropocene. *Science* **348**, aaa3716 (2015). doi: 10.1126/science.aaa3716; pmid: 25883362
3. A. H. Knoll, M. J. Follows, A bottom-up perspective on ecosystem change in Mesozoic oceans. *Proc. Biol. Sci.* **283**, 20161755 (2016). doi: 10.1098/rspb.2016.1755; pmid: 27798303
4. J. A. Goldbogen *et al*., Why whales are big but not bigger: Physiological drivers and ecological limits in the age of ocean giants. *Science* **366**, 1367–1372 (2019). doi: 10.1126/science.aax9044; pmid: 31831666
5. W. Gearty, C. R. McClain, J. L. Payne, Energetic tradeoffs control the size distribution of aquatic mammals. *Proc. Natl. Acad. Sci. U.S.A.* **115**, 4194–4199 (2018). doi: 10.1073/pnas.1712629115; pmid: 29581289
6. G. J. Slater, J. A. Goldbogen, N. D. Pyenson, Independent evolution of baleen whale gigantism linked to Plio-Pleistocene ocean dynamics. *Proc. Biol. Sci.* **284**, 20170546 (2017). doi: 10.1098/rspb.2017.0546; pmid: 28539520
7. B. C. Moon, T. L. Stubbs, Early high rates and disparity in the evolution of ichthyosaurs. *Commun. Biol.* **3**, 68 (2020). doi: 10.1038/s42003-020-0779-6; pmid: 32054967
8. N. B. Fröbisch, J. Fröbisch, P. M. Sander, L. Schmitz, O. Rieppel, Macropredatory ichthyosaur from the Middle Triassic and the origin of modern trophic networks. *Proc. Natl. Acad. Sci. U.S.A.* **110**, 1393–1397 (2013). doi: 10.1073/pnas.1216750110; pmid: 23297200
9. P. M. Hull, Emergence of modern marine ecosystems. *Curr. Biol.* **27**, R466–R469 (2017). doi: 10.1016/j.cub.2017.04.041; pmid: 28586680
10. See supplementary materials.
11. C. v. Linnaeus, *Systema Naturae. Regnum Animale* (L. Salvius, Stockholm, ed. 10, 1758).
12. H. F. Osborn, The reptilian subclasses Diapsida and Synapsida and the early history of the Diaptosauria. *Mem. Am. Mus. Nat. Hist.* **1**, 449–507 (1903).
13. H. M. D. de Blainville, Systéme de'Herpetologie. *Nouv. Ann. Mus. Hist. Nat. Paris* **4**, 233–296 (1835).
14. J. Leidy, Notice of some reptilian remains from Nevada. *Proc. Acad. Nat. Sci. Philadelphia* **20**, 177–178 (1868).
15. P. M. Sander, The large ichthyosaur *Cymbospondylus buchseri*, sp. nov., from the Middle Triassic of Monte San Giorgio (Switzerland), with a survey of the genus in Europe. *J. Vertebr. Paleontol.* **9**, 163–173 (1989). doi: 10.1080/02724634.1989.10011750
16. N. Fröbisch, P. M. Sander, O. Rieppel, A new species of *Cymbospondylus* (Diapsida, Ichthyosauria) from the Middle Triassic of Nevada and re-evaluation of the skull osteology of the genus. *Zool. J. Linn. Soc.* **147**, 515–538 (2006). doi: 10.1111/j.1096-3642.2006.00225.x
17. N. Klein, L. Schmitz, T. Wintrich, P. M. Sander, A new cymbospondylid ichthyosaur (Ichthyosauria) from the Middle Triassic (Anisian) of the Augusta Mountains, Nevada, USA. *J. Syst. Palaeontology* **18**, 1167–1191 (2020). doi: 10.1080/14772019.2020.1748132
18. C. Monnet, H. Bucher, New middle and late Anisian (Middle Triassic) ammonoid faunas from Northwestern Nevada (USA): Taxonomy and biochronology. *Foss. Strat.* **52**, 1–121 (2005).
19. B. Moon, A new phylogeny of ichthyosaurs (Reptilia: Diapsida). *J. Syst. Palaeontology* **17**, 129–155 (2019). doi: 10.1080/14772019.2017.1394922
20. J. A. Massare, Tooth morphology and prey preference of Mesozoic marine reptiles. *J. Vertebr. Paleontol.* **7**, 121–137 (1987). doi: 10.1080/02724634.1987.10011647
21. R. Motani, Evolution of fish-shaped reptiles (Reptilia: Ichthyopterygia) in their physical environments and constraints. *Annu. Rev. Earth Planet. Sci.* **33**, 12.11–12.26 (2005).
22. C. McGowan, Giant ichthyosaurs of the Early Jurassic. *Can. J. Earth Sci.* **33**, 1011–1021 (1996). doi: 10.1139/e96-077
23. T. M. Scheyer, C. Romano, J. Jenks, H. Bucher, Early Triassic marine biotic recovery: The predators' perspective. *PLOS ONE* **9**, e88987 (2014). doi: 10.1371/journal.pone.0088987; pmid: 24647136
24. S. Gutarra *et al*., Effects of body plan evolution on the hydrodynamic drag and energy requirements of swimming in ichthyosaurs. *Proc. Biol. Sci.* **286**, 20182786 (2019). doi: 10.1098/rspb.2018.2786; pmid: 30836867
25. R. Motani *et al*., A basal ichthyosauriform with a short snout from the Lower Triassic of China. *Nature* **517**, 485–488 (2015). doi: 10.1038/nature13866; pmid: 25383536
26. S. Nummela, T. Hussain, J. G. M. Thewissen, Cranial anatomy of Pakicetidae (Cetacea, Mammalia). *J. Vertebr. Paleontol.* **26**, 746–759 (2006). doi: 10.1671/0272-4634(2006)26[746:CAOPCM]2.0.CO;2
27. J. G. M. Thewissen, J. D. Sensor, M. T. Clementz, S. Bajpai, Evolution of dental wear and diet during the origin of whales. *Paleobiology* **37**, 655–669 (2011). doi: 10.1666/10038.1
28. M. A. MacIver, L. Schmitz, U. Mugan, T. D. Murphey, C. D. Mobley, Massive increase in visual range preceded the origin of terrestrial vertebrates. *Proc. Natl. Acad. Sci. U.S.A.* **114**, E2375–E2384 (2017). doi: 10.1073/pnas.1615563114; pmid: 28270619
29. J. M. Fahlke, K. A. Bastl, G. M. Semprebon, P. D. Gingerich, Paleoecology of archaeocete whales throughout the Eocene: Dietary adaptations revealed by microwear analysis. *Palaeogeogr. Palaeoclimatol. Palaeoecol.* **386**, 690–701 (2013). doi: 10.1016/j.palaeo.2013.06.032
30. L. N. Cooper *et al*., Aquatic habits of cetacean ancestors: Integrating bone microanatomy and stable isotopes. *Integr. Comp. Biol.* **56**, 1370–1384 (2016). doi: 10.1093/icb/icw119; pmid: 27697778
31. L. J. Revell, Phytools: An R package for phylogenetic comparative biology (and other things). *Methods Ecol. Evol.* **3**, 217–223 (2012). doi: 10.1111/j.2041-210X.2011.00169.x
32. J. C. Uyeda, L. J. Harmon, A novel Bayesian method for inferring and interpreting the dynamics of adaptive landscapes from phylogenetic comparative data. *Syst. Biol.* **63**, 902–918 (2014). doi: 10.1093/sysbio/syu057; pmid: 25077513
33. C. M. Peredo, N. D. Pyenson, C. D. Marshall, M. D. Uhen, Tooth loss precedes the origin of baleen in whales. *Curr. Biol.* **28**, 3992–4000.e2 (2018). doi: 10.1016/j.cub.2018.10.047; pmid: 30503622
34. J. D. Walker, J. W. Geissman, S. A. Bowring, L. E. Babcock, "Geologic time scale v. 5.0" (Geological Society of America, 2018).
35. K. M. Nichols, N. J. Silberling, Stratigraphy and depositional history of the Star Peak Group (Triassic), northwestern Nevada. *Spec. Pap. Geol. Soc. Am.* **178**, 1–73 (1977).
36. G. Cuny, O. Rieppel, P. M. Sander, The shark fauna from the Middle Triassic (Anisian) of North-Western Nevada. *Zool. J. Linn. Soc.* **133**, 285–301 (2001). doi: 10.1111/j.1096-3642.2001.tb00627.x
37. O. Rieppel, *Handbook of Paleoherpetology / Sauropterygia I.: Placodontia, Pachypleurosauria, Nothosauroidea, Pistosauroidea* (Friedrich Pfeil, 2000).
38. J. C. Merriam, *Triassic Ichthyosauria, with Special Reference to the American Forms* (Memoirs of the University of California, The University Press, 1908).
39. L. Schmitz, P. M. Sander, G. W. Storrs, O. Rieppel, New Mixosauridae (Ichthyosauria) from the Middle Triassic of the Augusta Mountains (Nevada, USA) and their implications for mixosaur taxonomy. *Palaentographica A* **270**, 133–162 (2004).
40. J. C. Merriam, Preliminary note on a new marine reptile from the Middle Triassic of Nevada. *Univ. Calif. Publication Bull. Dept. Geol.* **5**, 5–79 (1906).
41. B. Gauzens *et al*., Fluxweb: An R package to easily estimate energy fluxes in food webs. *Methods Ecol. Evol.* **10**, 270–279 (2018). doi: 10.1111/2041-210X.13109
42. N. D. Martinez, Allometric trophic networks from individuals to socio-ecosystems: Consumer-resource theory of the ecological elephant in the room. *Front. Ecol. Evol.* **8**, 92 (2020). doi: 10.3389/fevo.2020.00092
43. R. Motani, D.-Y. Jiang, A. Tintori, C. Ji, J.-D. Huang, Pre- versus post-mass extinction divergence of Mesozoic marine reptiles dictated by time-scale dependence of evolutionary rates. *Proc. Biol. Sci.* **284**, 20170241 (2017). doi: 10.1098/rspb.2017.0241; pmid: 28515201
44. J. H. Brown, J. F. Gillooly, A. P. Allen, V. M. Savage, G. B. West, Toward a metabolic theory of ecology. *Ecology* **85**, 1771–1789 (2004). doi: 10.1890/03-9000
45. E. L. Nicholls, M. Manabe, Giant ichthyosaurs of the Triassic – A new species of *Shonisaurus* from the Pardonet Formation (Norian, Late Triassic) of British Columbia. *J. Vertebr. Paleontol.* **24**, 838–849 (2004). doi: 10.1671/0272-4634(2004)024[0838:GIOTTN]2.0.CO;2
46. C. R. McClain *et al*., Sizing ocean giants: Patterns of intraspecific size variation in marine megafauna. *PeerJ* **3**, e715 (2015). doi: 10.7717/peerj.715; pmid: 25649000
47. A. Brayard *et al*., Unexpected Early Triassic marine ecosystem and the rise of the Modern evolutionary fauna. *Sci. Adv.* **3**,

e1602159 (2017). doi: 10.1126/sciadv.1602159; pmid: 28246643
48. H. Song, P. B. Wignall, A. M. Dunhill, Decoupled taxonomic and ecological recoveries from the Permo-Triassic extinction. *Sci. Adv.* **4**, eaat5091 (2018). doi: 10.1126/sciadv.aat5091; pmid: 30324133
49. P. M. Sander *et al*., Biology of the sauropod dinosaurs: The evolution of gigantism. *Biol. Rev. Camb. Philos. Soc.* **86**, 117–155 (2011). doi: 10.1111/j.1469-185X.2010.00137.x; pmid: 21251189
50. M. J. Benton *et al*., Exceptional vertebrate biotas from the Triassic of China, and the expansion of marine ecosystems after the Permo-Triassic mass extinction. *Earth Sci. Rev.* **137**, 85–128 (2014). doi: 10.1016/j.earscirev.2014.08.004
51. M. J. Orchard, Conodont diversity and evolution through the latest Permian and Early Triassic upheavals. *Palaeogeogr. Palaeoclimatol. Palaeoecol.* **252**, 93–117 (2007). doi: 10.1016/j.palaeo.2006.11.037
52. R. Motani, B. M. Rothschild, W. J. Wahl Jr., Large eyeballs in diving ichthyosaurs. *Nature* **402**, 747 (1999). doi: 10.1038/45435
53. D.-E. Nilsson, E. Warrant, S. Johnsen, Computational visual ecology in the pelagic realm. *Philos. Trans. R. Soc. London Ser. B* **369**, 20130038 (2014). doi: 10.1098/rstb.2013.0038; pmid: 24395965
54. J. M. Grady *et al*., Metabolic asymmetry and the global diversity of marine predators. *Science* **363**, eaat4220 (2019). doi: 10.1126/science.aat4220; pmid: 30679341
55. C. Pimiento, J. L. Cantalapiedra, K. Shimada, D. J. Field, J. B. Smaers, Evolutionary pathways toward gigantism in sharks and rays. *Evolution* **73**, 588–599 (2019). doi: 10.1111/evo.13680; pmid: 30675721
56. A. T. Boersma, N. D. Pyenson, *Albicetus oxymycterus*, a new generic name and redescription of a basal physeteroid (Mammalia, Cetacea) from the Miocene of California, and the evolution of body size in sperm whales. *PLOS ONE* **10**, e0135551 (2015). doi: 10.1371/journal.pone.0135551; pmid: 26651027
57. R. W. Boessenecker, M. Churchill, E. A. Buchholtz, B. L. Beatty, J. H. Geisler, Convergent evolution of swimming adaptations in modern whales revealed by a large macrophagous dolphin from the Oligocene of South Carolina. *Curr. Biol.* **30**, 3267–3273.e2 (2020). doi: 10.1016/j.cub.2020.06.012; pmid: 32649912
58. J. H. Geisler, M. W. Colbert, J. L. Carew, A new fossil species supports an early origin for toothed whale echolocation. *Nature* **508**, 383–386 (2014). doi: 10.1038/nature13086; pmid: 24670659
59. J. A. Goldbogen, P. T. Madsen, The evolution of foraging capacity and gigantism in cetaceans. *J. Exp. Biol.* **221**, jeb166033 (2018). doi: 10.1242/jeb.166033; pmid: 29895582
60. E. E. Maxwell, D. Y. Cortés, P. Patarroyo, M. L. P. Ruge, A new specimen of *Platypterygius sachicarum* (Reptilia, Ichthyosauria) from the Early Cretaceous of Colombia and its phylogenetic implications. *J. Vertebr. Paleontol.* **39**, e1577875 (2019). doi: 10.1080/02724634.2019.1577875
61. W. P. Maddison, D. R. Maddison, Mesquite: A modular system for evolutionary analysis. Version 3.02 (2015); www.mesquiteproject.org.
62. P. A. Goloboff, J. S. Farris, K. C. Nixon, TNT, a free program for phylogenetic analysis. *Cladistics* **24**, 774–786 (2008). doi: 10.1111/j.1096-0031.2008.00217.x
63. J.-D. Huang *et al*., The new ichthyosauriform *Chaohusaurus brevifemoralis* (Reptilia, Ichthyosauromorpha) from Majiashan, Chaohu, Anhui Province, China. *PeerJ* **7**, e7561 (2019). doi: 10.7717/peerj.7561; pmid: 31565558
64. D. Swofford, *PAUP*. Phylogenetic Analysis Using Parsimony (* and Other Methods). Version 4.0b10* (Sinauer Associates, 2002).
65. R Core Team, R software, version 3.5.2 (R Foundation for Statistical Computing, Vienna, Austria, 2020); www.R-project.org/.
66. J. H. Geisler, A. E. Sanders, Morphological evidence for the phylogeny of Cetacea. *J. Mamm. Evol.* **10**, 23–129 (2003). doi: 10.1023/A:1025552007291
67. G. T. Lloyd, G. J. Slater, A total-group phylogenetic metatree for Cetacea and the importance of fossil data in diversification analyses. *Syst. Biol.* **70**, 922–939 (2021). doi: 10.1093/sysbio/syab002; pmid: 33507304
68. S. Bajpai, P. D. Gingerich, A new Eocene archaeocete (Mammalia, Cetacea) from India and the time of origin of whales. *Proc. Natl. Acad. Sci. U.S.A.* **95**, 15464–15468 (1998). doi: 10.1073/pnas.95.26.15464; pmid: 9860991
69. A. E. Hernández Cisneros, J. Velez-Juarbe, Paleobiogeography of the North Pacific toothed mysticetes (Cetacea: Aetiocetidae): A key on the Oligocene cetacean distributional patterns. *Palaeontology* **64**, 51–61 (2021). doi: 10.1111/pala.12507
70. M. Viglino, M. R. Buono, R. E. Fordyce, J. I. Cuitiño, E. M. G. Fitzgerald, Anatomy and phylogeny of the large shark-toothed dolphin *Phoberodon arctirostris* Cabrera, 1926 (Cetacea: Odontoceti) from the early Miocene of Patagonia (Argentina). *Zool. J. Linn. Soc.* **185**, 511–542 (2019). doi: 10.1093/zoolinnean/zly053
71. C. M. Peredo, M. D. Uhen, M. D. Nelson, A new kentriodontid (Cetacea: Odontoceti) from the early Miocene Astoria Formation and a revision of the stem delphinidan family Kentriodontidae. *J. Vertebr. Paleontol.* **38**, e1411357 (2018). doi: 10.1080/02724634.2017.1411357
72. M. R. McGowen *et al*., Phylogenomic resolution of the cetacean tree of life using target sequence capture. *Syst. Biol.* **69**, 479–501 (2020). doi: 10.1093/sysbio/syz068; pmid: 31633766
73. N. D. Pyenson, S. N. Sponberg, Reconstructing body size in extinct crown Cetacea (Neoceti) using allometry, phylogenetic methods and tests from the fossil record. *J. Mamm. Evol.* **18**, 269–288 (2011). doi: 10.1007/s10914-011-9170-1
74. N. Cooper, G. H. Thomas, C. Venditti, A. Meade, R. P. Freckleton, A cautionary note on the use of Ornstein Uhlenbeck models in macroevolutionary studies. *Biol. J. Linn. Soc. Lond.* **118**, 64–77 (2016). doi: 10.1111/bij.12701; pmid: 27478249
75. D. L. Pisor, *Registry of World Record Size Shells* (ConchBooks, ed. 5, 2008).

ACKNOWLEDGMENTS

We thank D. Goodreau and E. Durazo [all from Dinosaur Institute (DI), Natural History Museum of Los Angeles County (LACM)] for preparation of the specimen; M. Walsh (DI) for curation; and S. Abramowicz (DI) and G. Oleschinski (Bonn) for photography. S. Abramowicz is acknowledged for drafting the summary figure. E. Maxwell (Stuttgart) kindly made the data matrix from (*60*) available before final publication and provided helpful technical advice. The specimen was collected under Bureau of Land Management (BLM) Paleontological Resources Use Permit N-92625. The help of BLM staff at the Winnemucca field office is gratefully acknowledged. We thank the reviewers for their constructive comments. T. and B. Young and their Great Basin Brewery (Reno, NV, USA) generously supported our fieldwork by contributions in kind and monetary contributions. **Funding:** This research was funded in part by grants from the Deutsche Forschungsgemeinschaft (project numbers 388659338 and 264173172) to P.M.S. and by the National Geographic Society (grant number 9599-14) and the W. M. Keck Science Department to L.S. Great Basin Brewery (Reno, NV) supported our fieldwork and the preparation of the specimen at the LACM. Additional support was provided by the DI under the direction of L. Chiappe. The work of L.J.R. on phytools is supported by the National Science Foundation (DEB-1350474 and DBI-1759940). **Author contributions:** The overall idea, concept, and approach were developed by P.M.S., L.S., and T.W. Morphological descriptions and phylogenetic analysis were performed by P.M.S., N.K., T.W., and L.S. Evolutionary rate analysis was performed by L.S., J.V.J., and L.J.R. Energy-flux modeling was performed by E.M.G., N.K., and P.M.S. The manuscript was written by P.M.S. and L.S. with contributions from E.M.G., J.V.J., L.J.R., N.K., and T.W. All authors read, edited, and discussed the manuscript and participated in data collection. **Competing interests:** The authors declare no competing interests. **Data and materials availability:** The holotype specimen of *C. youngorum* sp. nov. is owned by the US Department of the Interior and housed in the collections of the Dinosaur Institute, Natural History Museum of Los Angeles County (Los Angeles, CA, USA) as LACM DI 157871. All data analyzed in this study are available in the main text and supplementary materials. R scripts are available at data S6 and S8.

SUPPLEMENTARY MATERIALS

science.org/doi/10.1126/science.abf5787
Supplementary Text
Figs. S1 to S21
Tables S1 to S14
References (*76*–*178*)
MDAR Reproducibility Checklist
Data S1 to S8

6 November 2020; accepted 26 October 2021
10.1126/science.abf5787